

**Sources of beam halo formation in
heavy-ion superconducting linac and
development of halo cleaning
methods**

**HALO'03
Montauk, NY**

Petr Ostroumov
May 20, 2003

Argonne National Laboratory
Operated by The University of Chicago
for the U.S. Department of Energy



Heavy-Ion Beam Dynamics in the RIA Accelerators

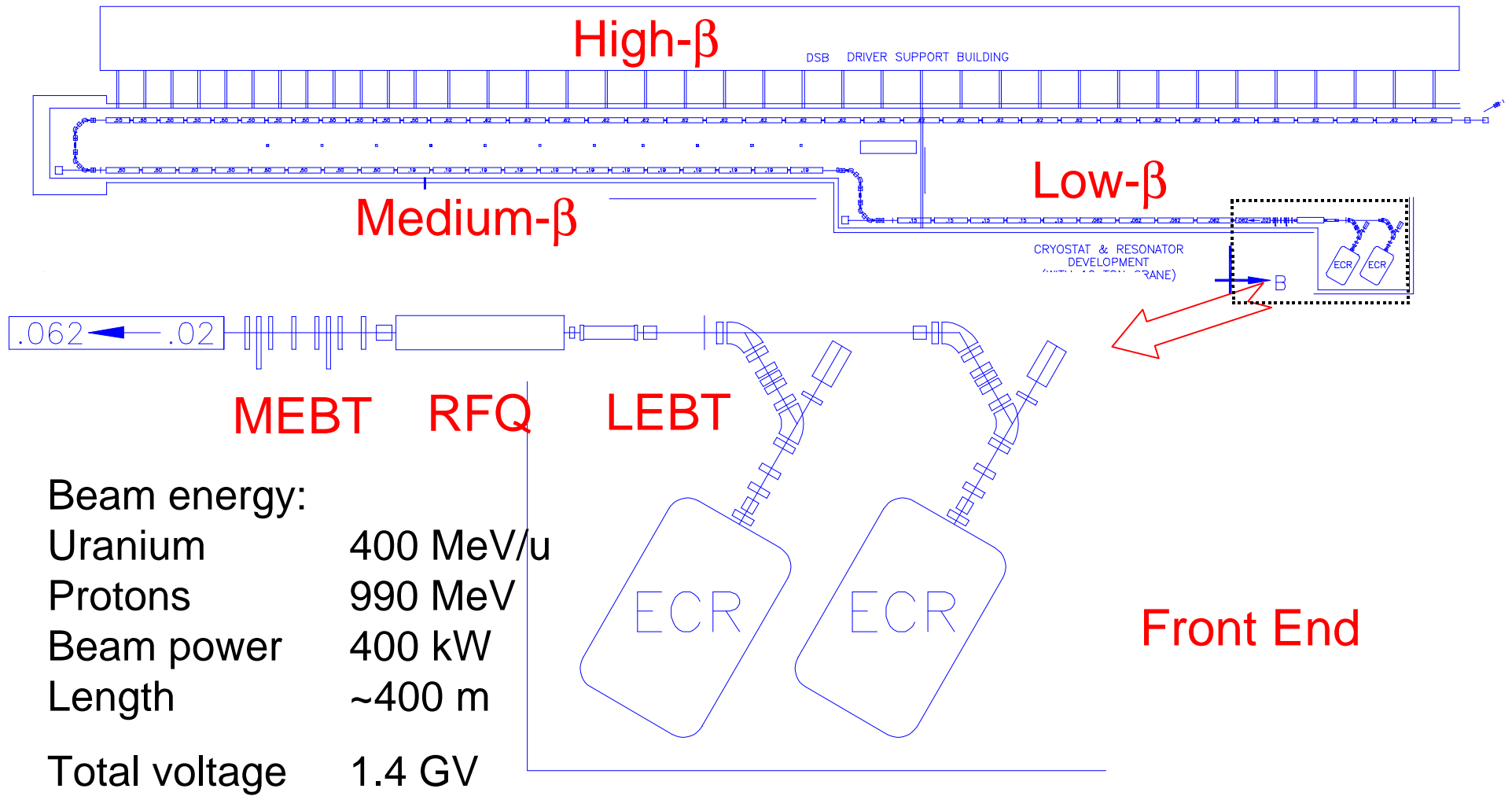
Acceleration of multiple-charge state heavy-ion beams.

The RIA Driver Linac:

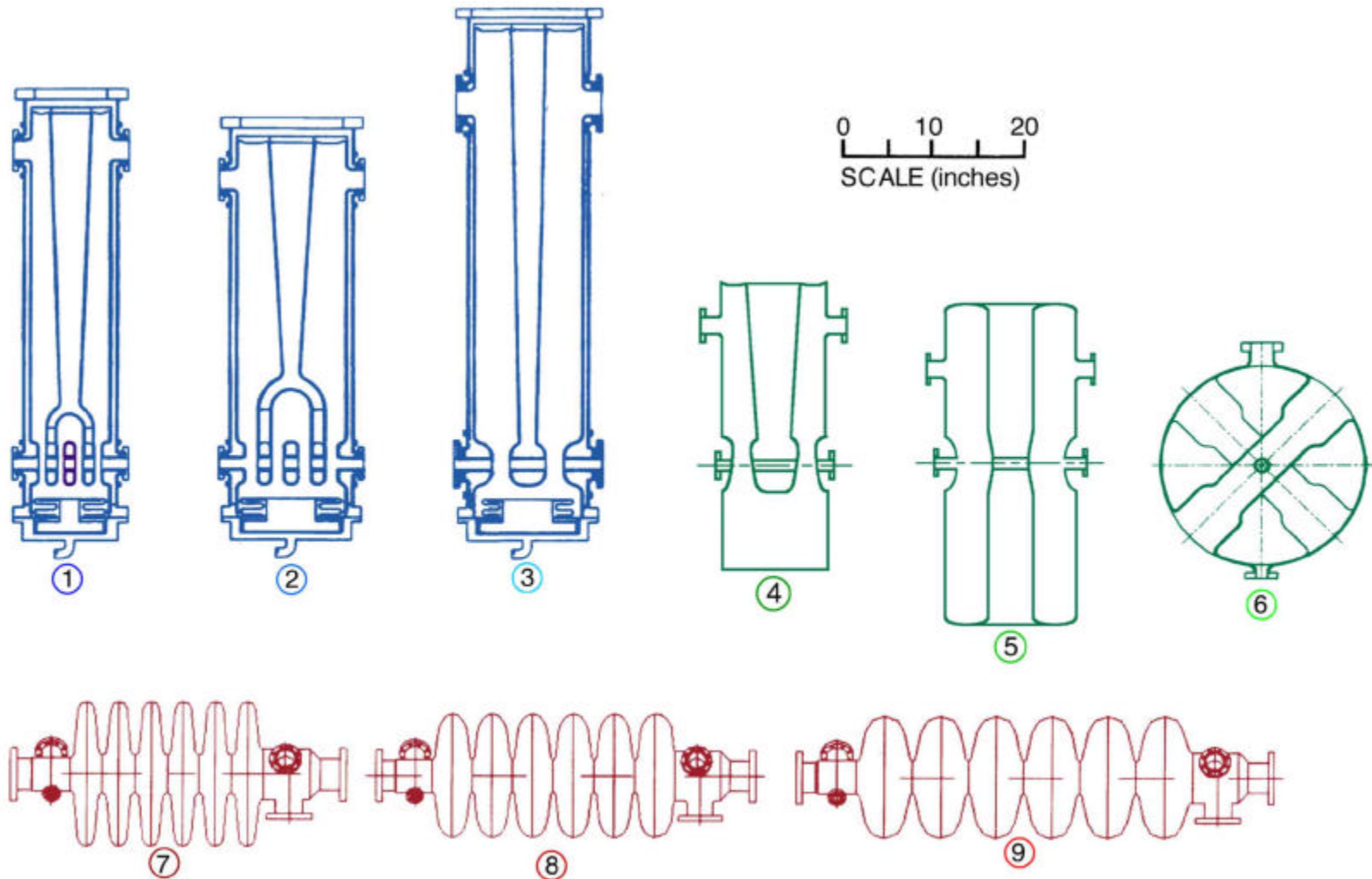
- Accelerating-Focusing Lattice of the SC linac;
- Beam Dynamics optimization and simulation;
- SRIM transport of 85 MeV/u uranium beam through 15 mg/cm² carbon foil. Properties of the energy-angle distribution.
- Post-stripper beam transport and acceleration in ECL and TSL.
- Beam collimation.
- Beam measurements at 10.5 MeV/u, comparison with SRIM calculations.
- BD simulations of the beam with larger σ in energy distribution.

Summary.

Driver Linac Architecture



SC Cavities for the RIA Driver



Main sources of longitudinal emittance growth&halo formation:

- Coupling of r-z motion in the RFQ.
- Multiplicity of charge states (different synchronous phase, frequency jumps: 57.5 MHz 345 MHz/805 MHz);
- Random errors of rf field phase and amplitude;
- Passage through the stripper, energy straggling.

Main sources of transverse emittance growth&halo formation:

- Space charge, higher-order distortions in the LEBT;
- Coherent oscillations of multi-q beams due to the misalignment of focusing elements;
- Mismatch of multi-q beam;
- Higher-order distortions in the post-stripper transport systems;
- Passage through the stripper, scattering.

Additional sources:

- Nonlinear motion in the long. phase space due to the lattice;
- Higher-order terms in the beam transport systems due to the charge spread $\Delta q/q$;
- Dipole component of magnetic field in some types of SC resonators;
- Quadrupole component of defocusing electric field in some types of SC resonators;
- Single particle parametric resonance should be avoided.

Detailed BD simulations are necessary for:

- a) Cost-effective design of the linac;
- b) Quantitative comparison of beam quality in different options of the linac.

Optimization codes

TRACE,
TRANSPORT,
COSY, GIOS;
DESRFQ.

Electromagnetic Field calculations

CST Microwave Studio;
SIMION;
DESRFQ.

Simulation codes

TRACKv32
DYNAMION

Multi-Component Ion Beam Simulation Code TRACKv32:

- multiparticle simulation of multiple component ion beams in 6D phase space;
- 3D electromagnetic fields from MWS in rectangular mesh;
- Fringing fields of magnets and multipoles are included;
- Realistic fields in solenoids;
- Integration of equations of motion by Runge-Kutta method;
- Misalignments and random errors are included;
- Space charge of multiple component ion beams;
- Beam passage through stripping foils&films;

TRACK elements:

Any type of accelerating resonator with realistic 3D fields;

Solenoids;

Bending magnets with fringing fields;

Multipoles (quadrupoles, sextupoles,) with fringing fields;

RFQs;

Multi-harmonic bunchers;

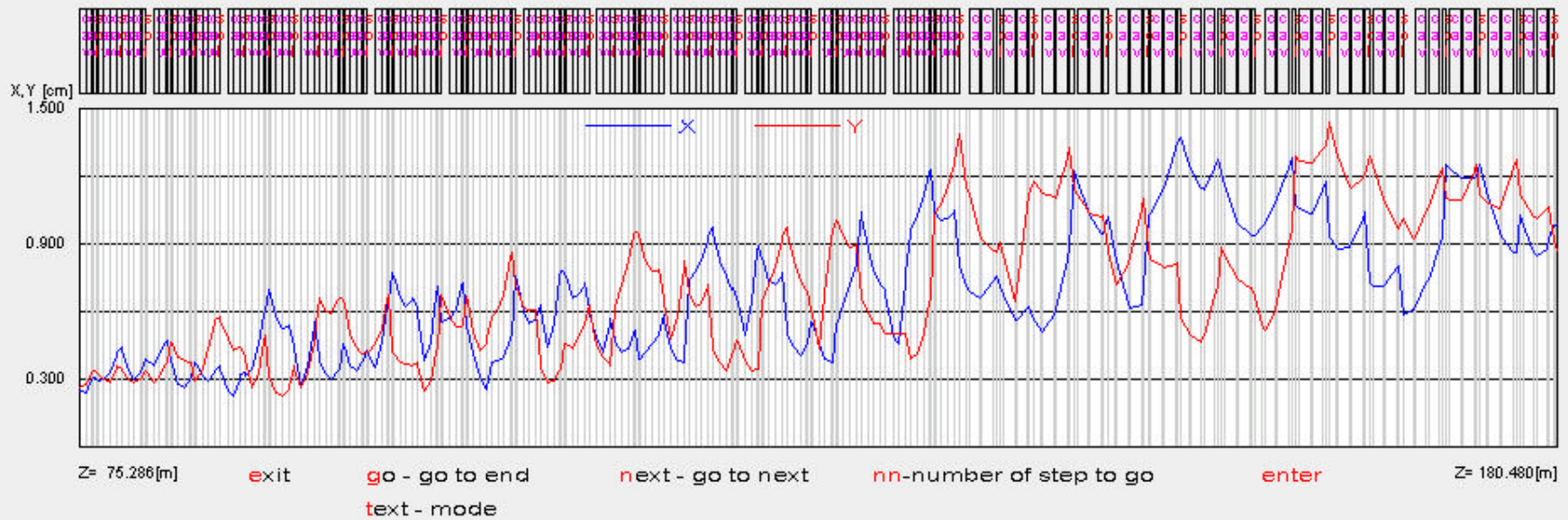
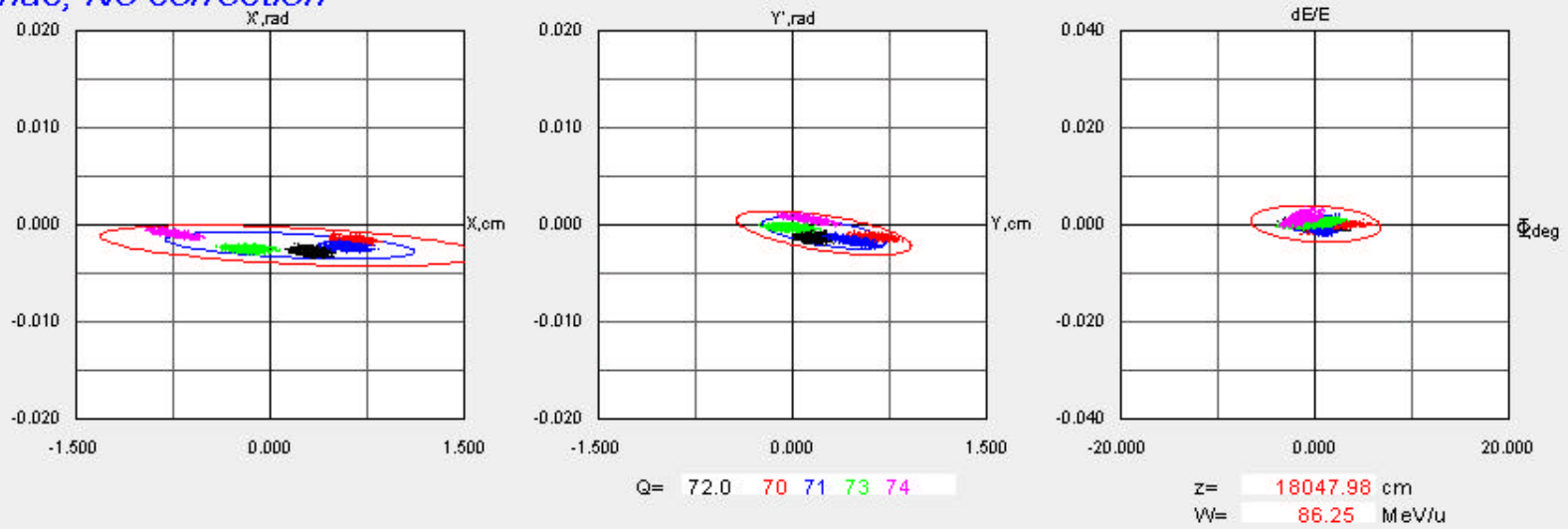
Axial-symmetric electrostatic lenses;

Change of electric potential (entrance/exit of HV deck);

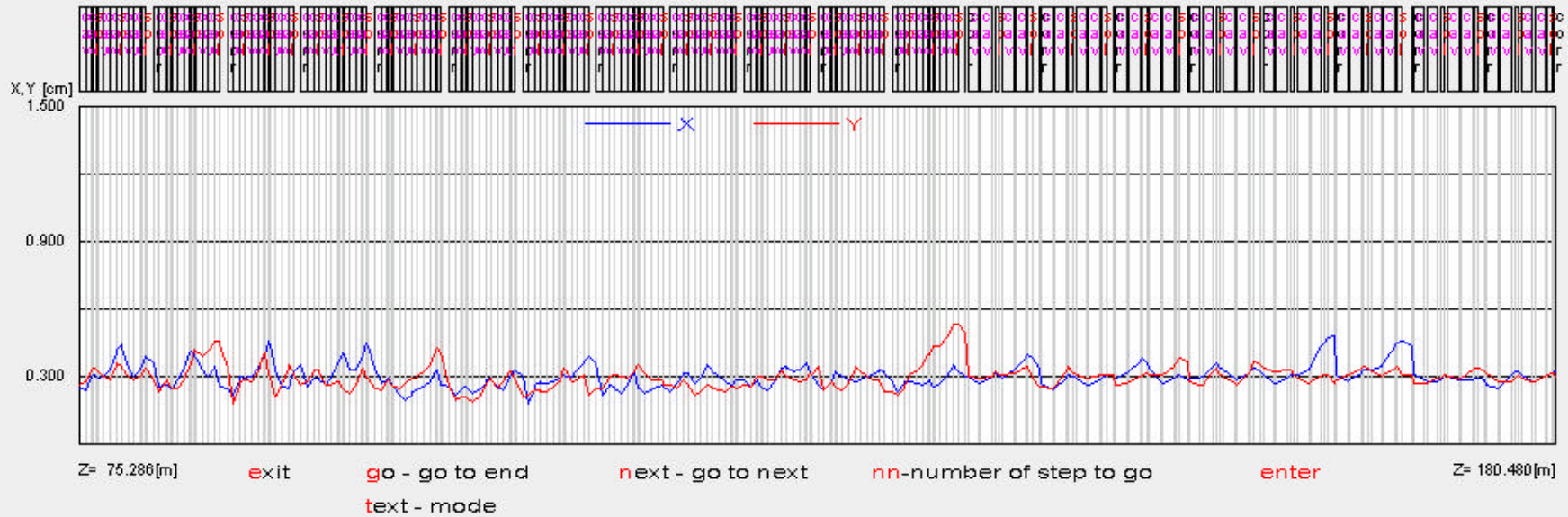
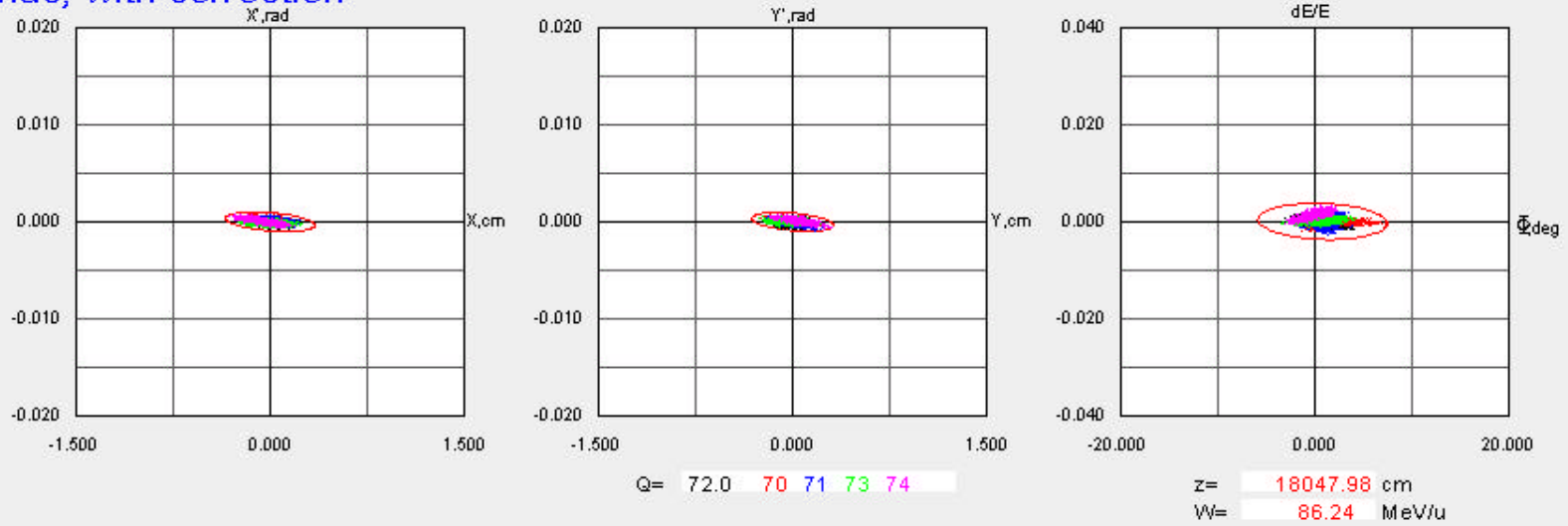
Thin beam steering elements;

Beam collimations element slit .

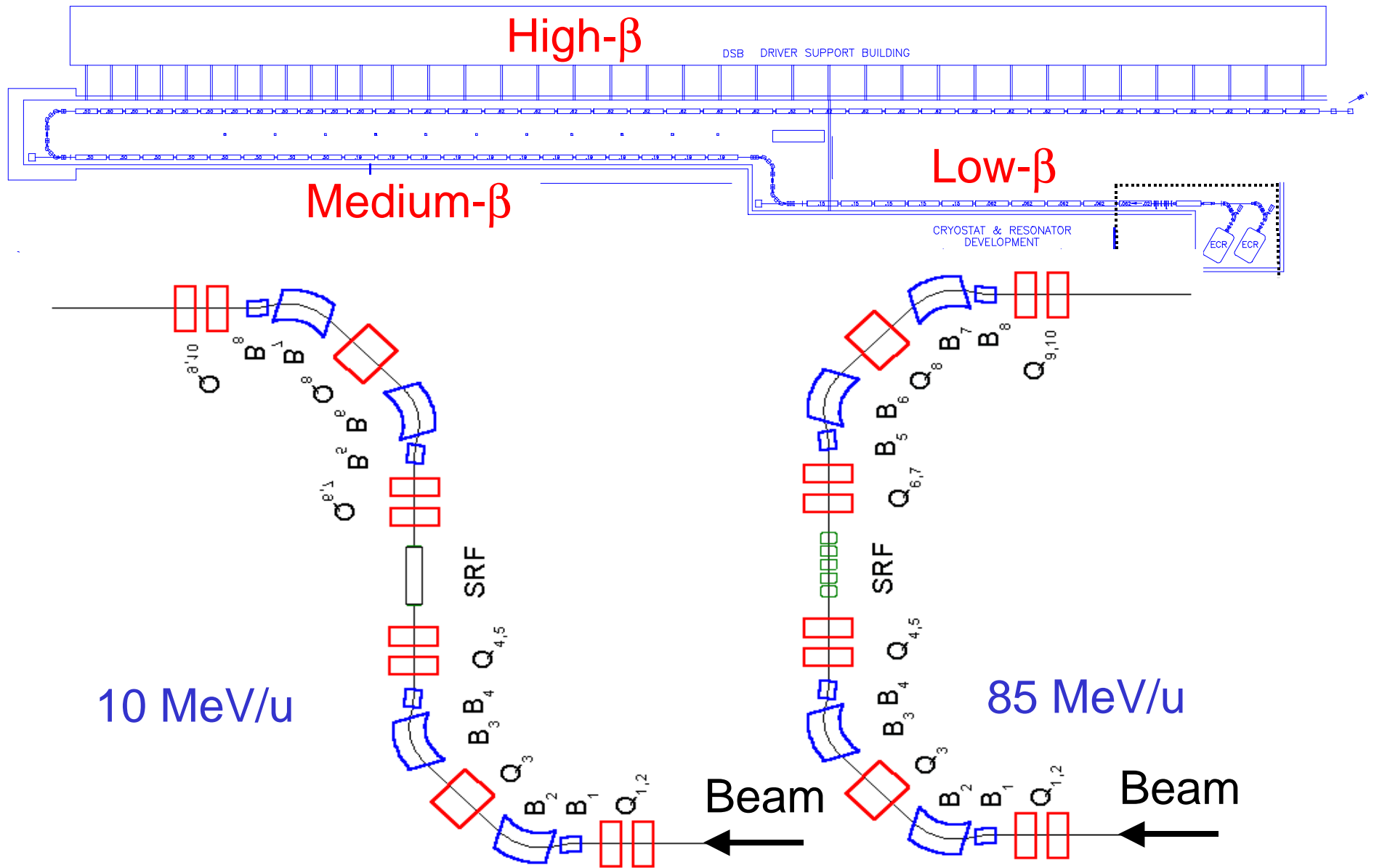
SC Linac, No correction



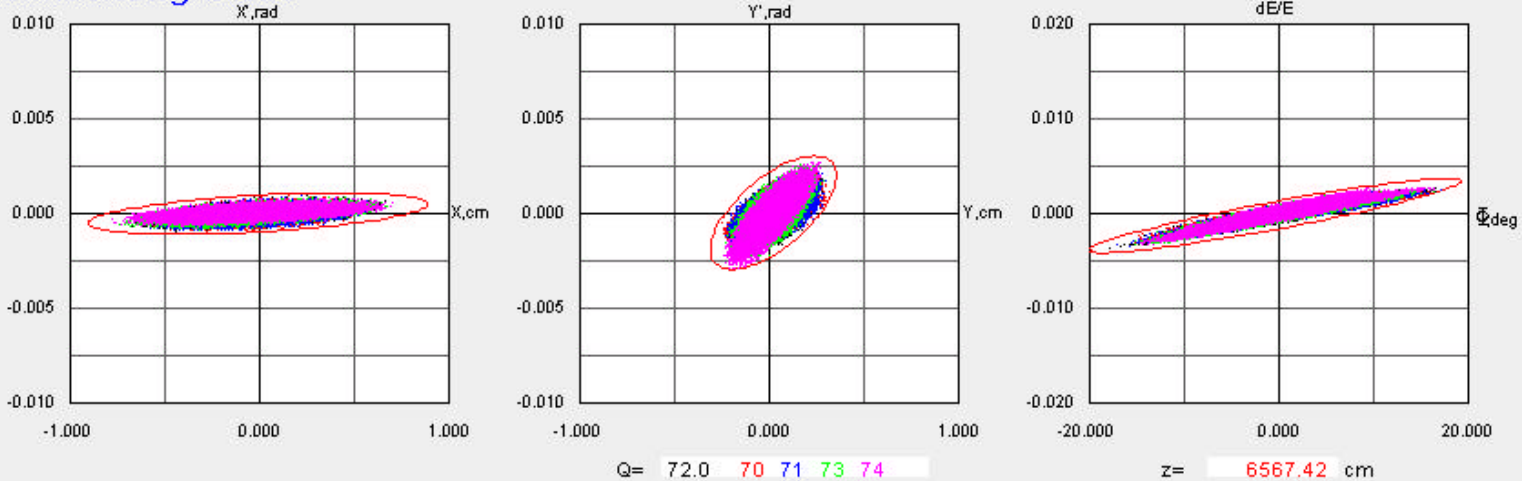
SC Linac, with correction



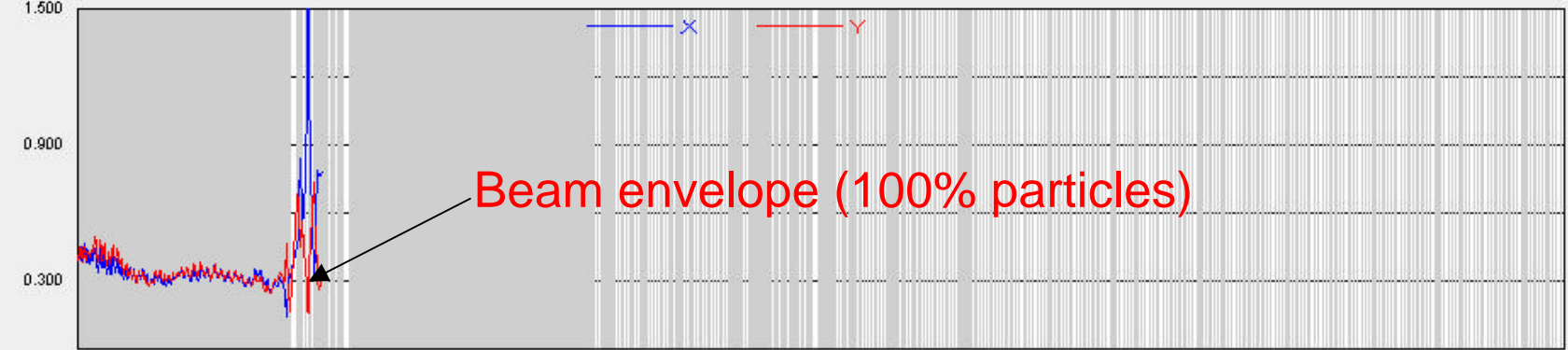
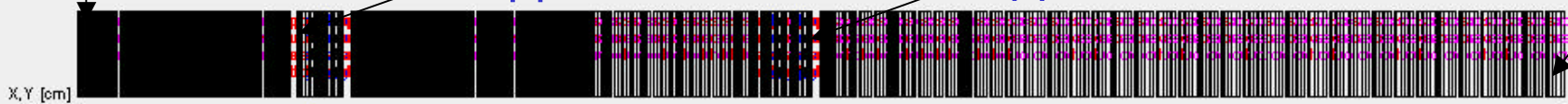
Driver Linac



Superconducting Linac



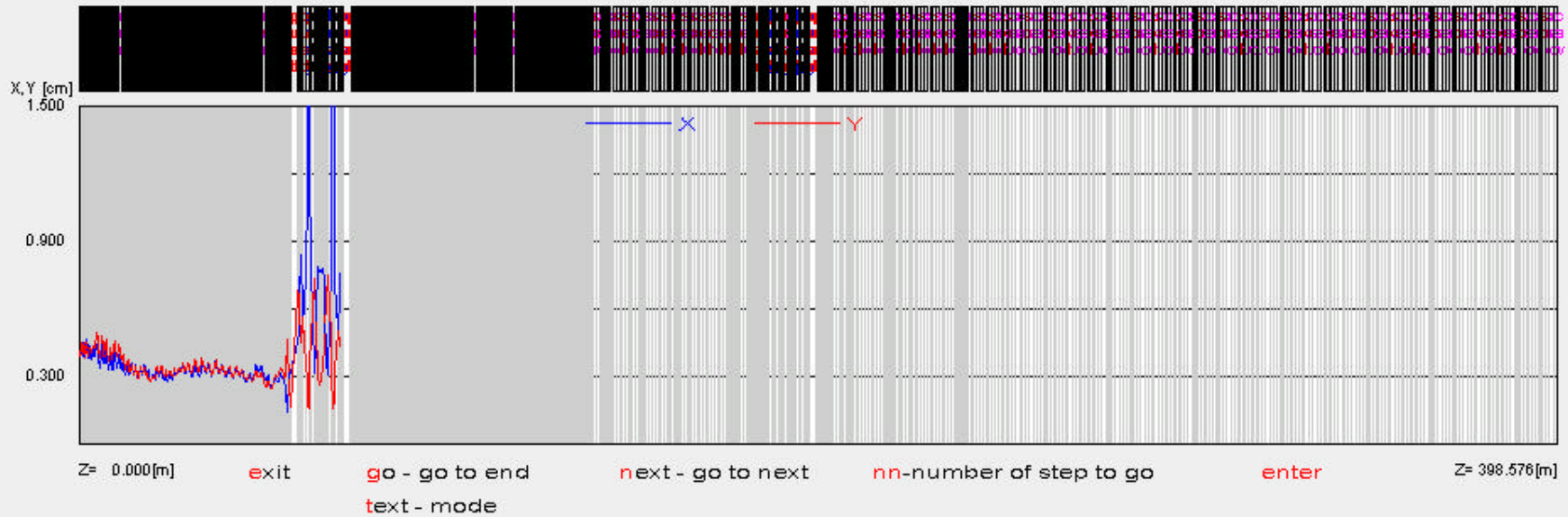
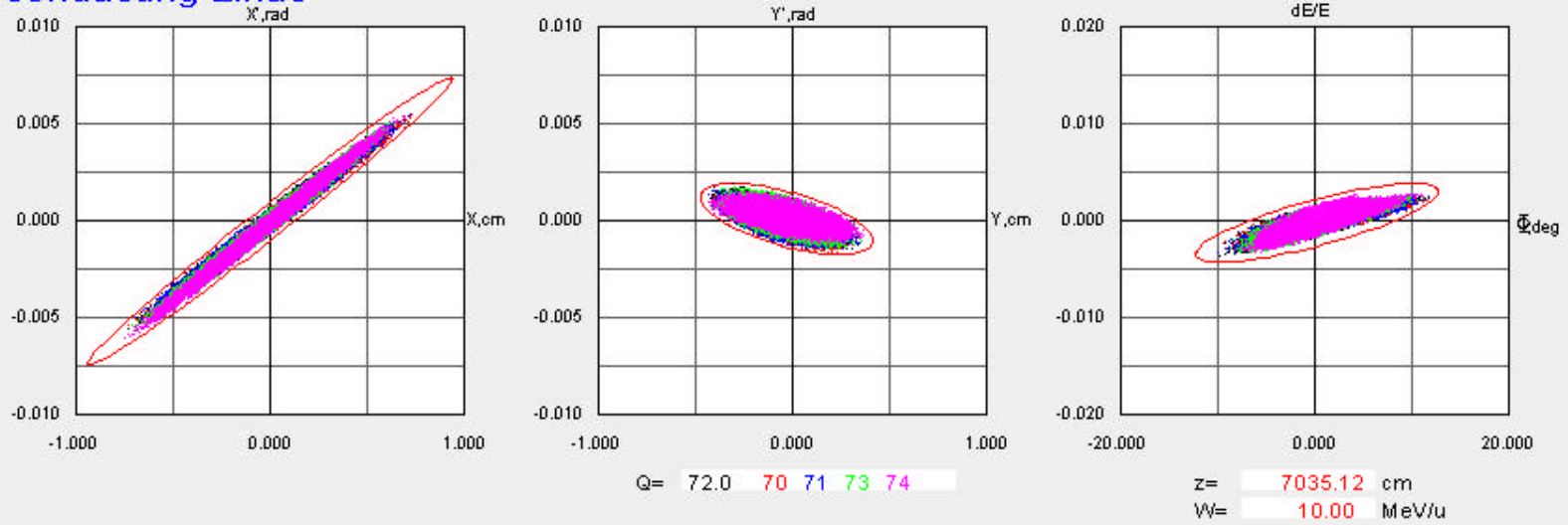
First SRF cavity
Stripper 1
Stripper 2
Last SRF cavity



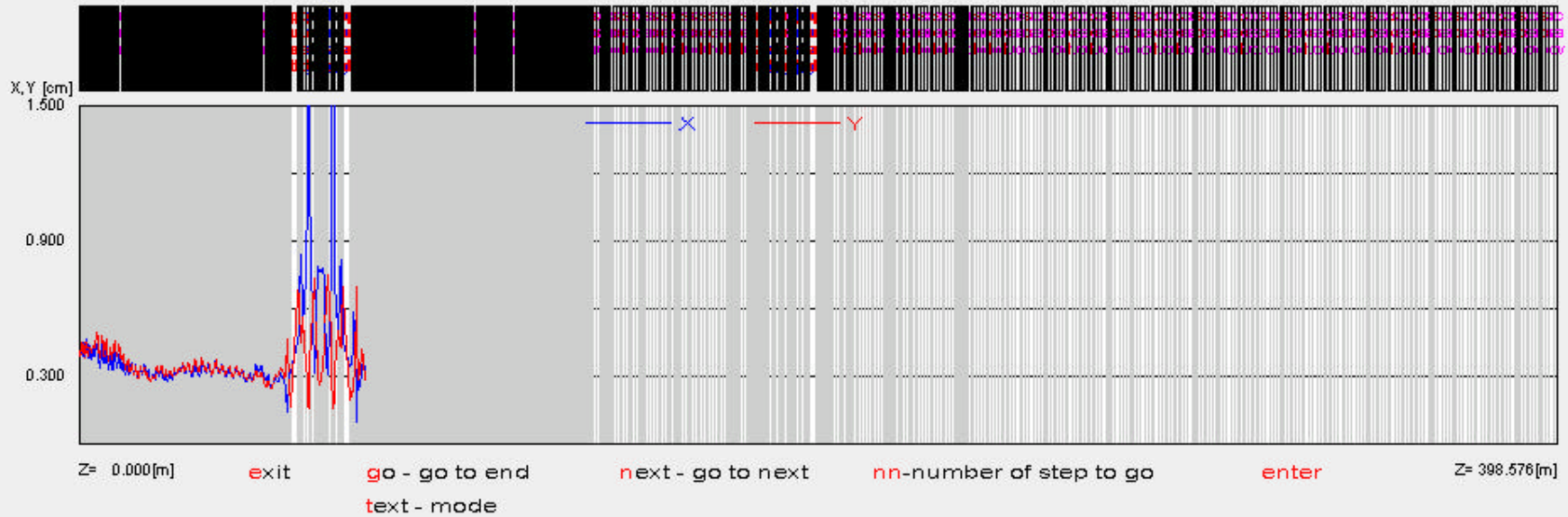
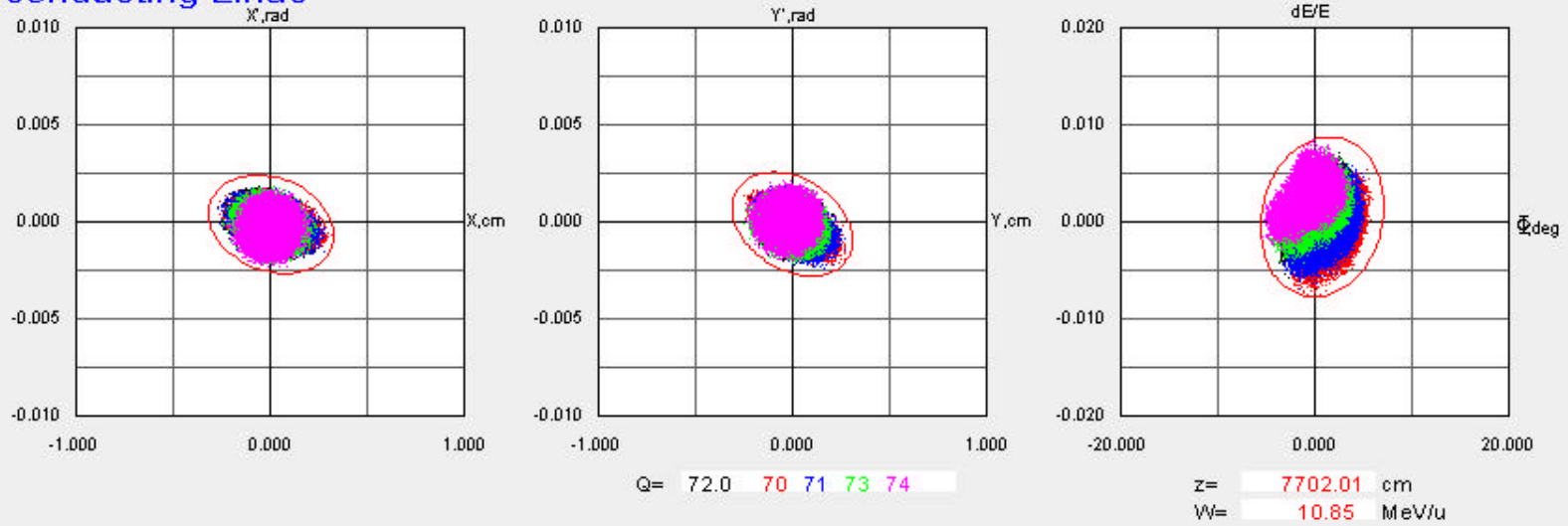
$Z = 0.000[m]$ exit go - go to end next - go to next nn - number of step to go enter $Z = 398.576[m]$
text - mode

Driver Linac with Triple Spoke Resonators

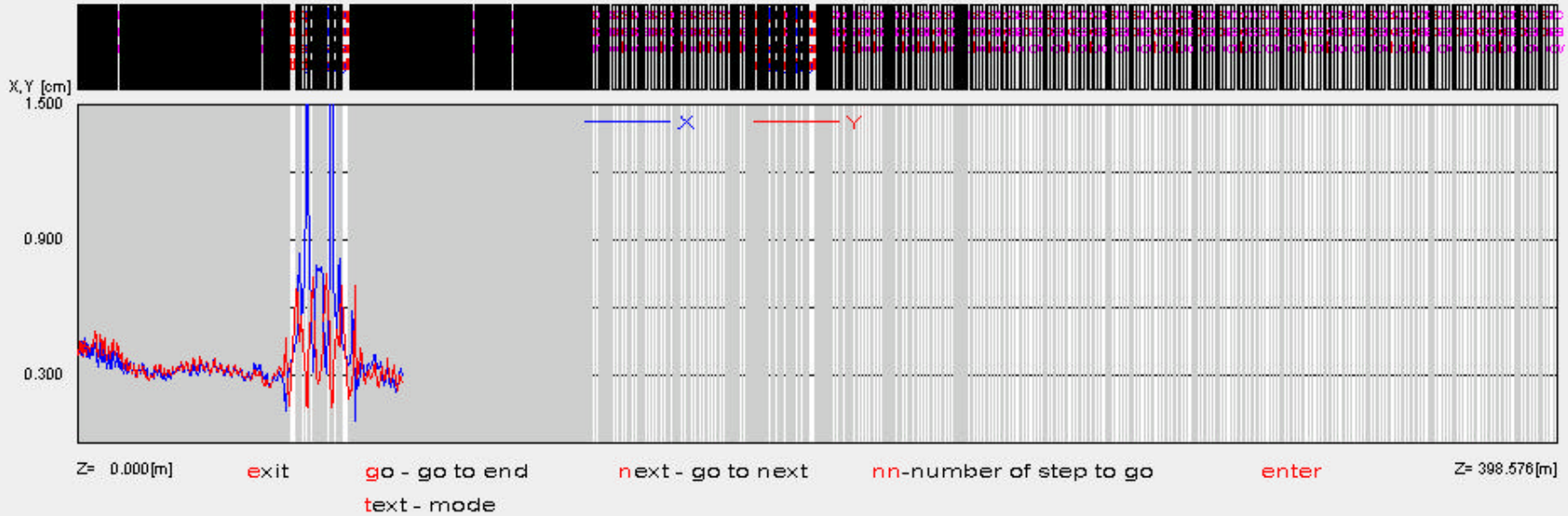
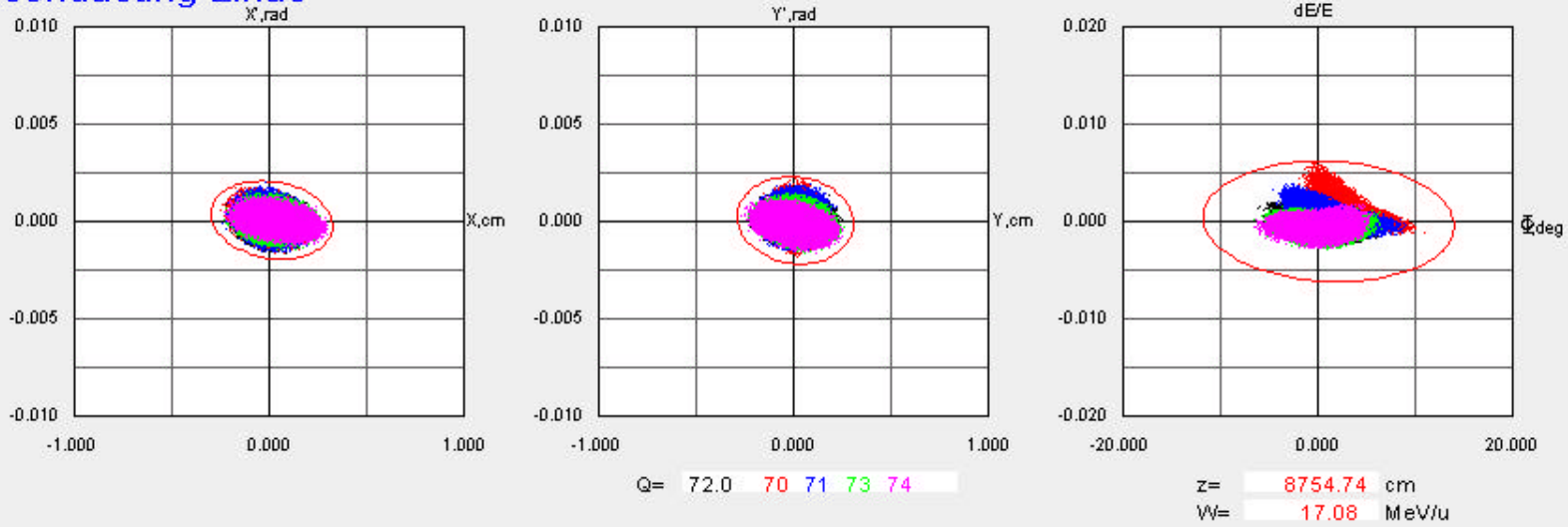
Superconducting Linac



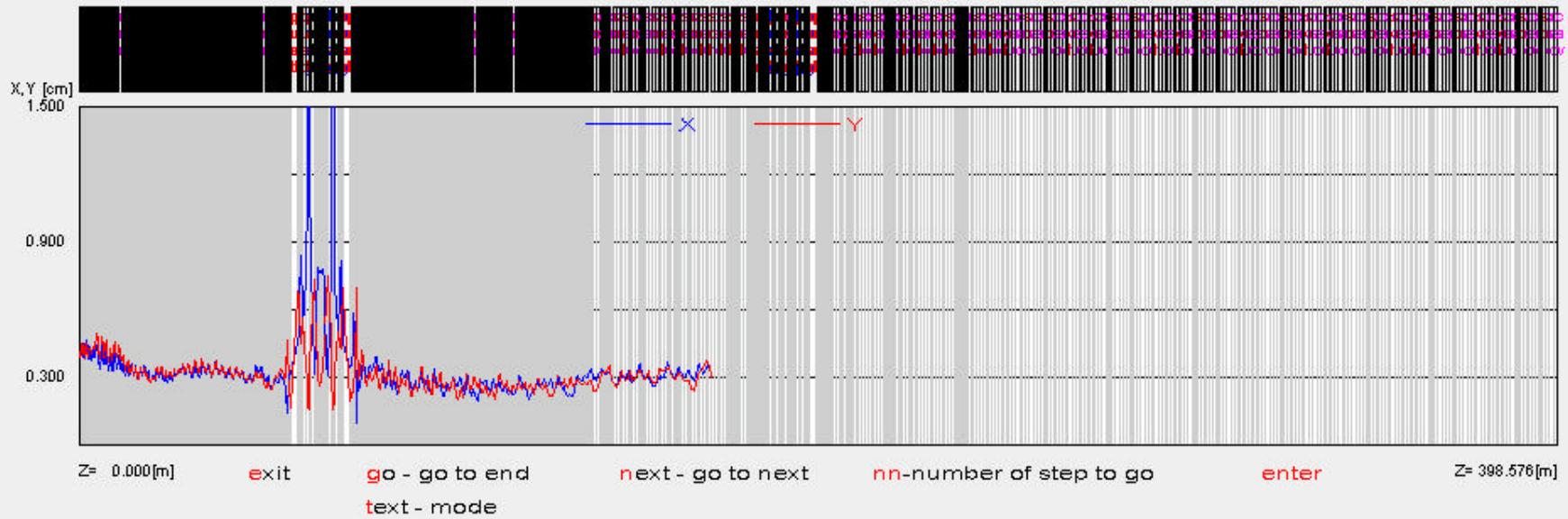
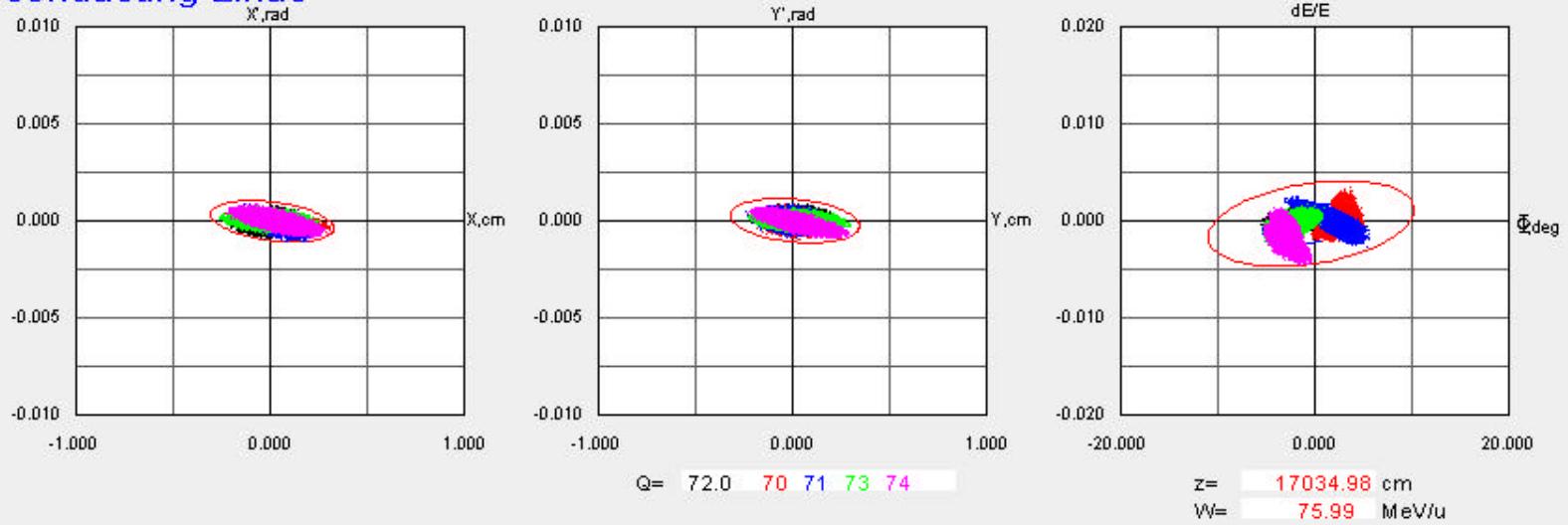
Superconducting Linac



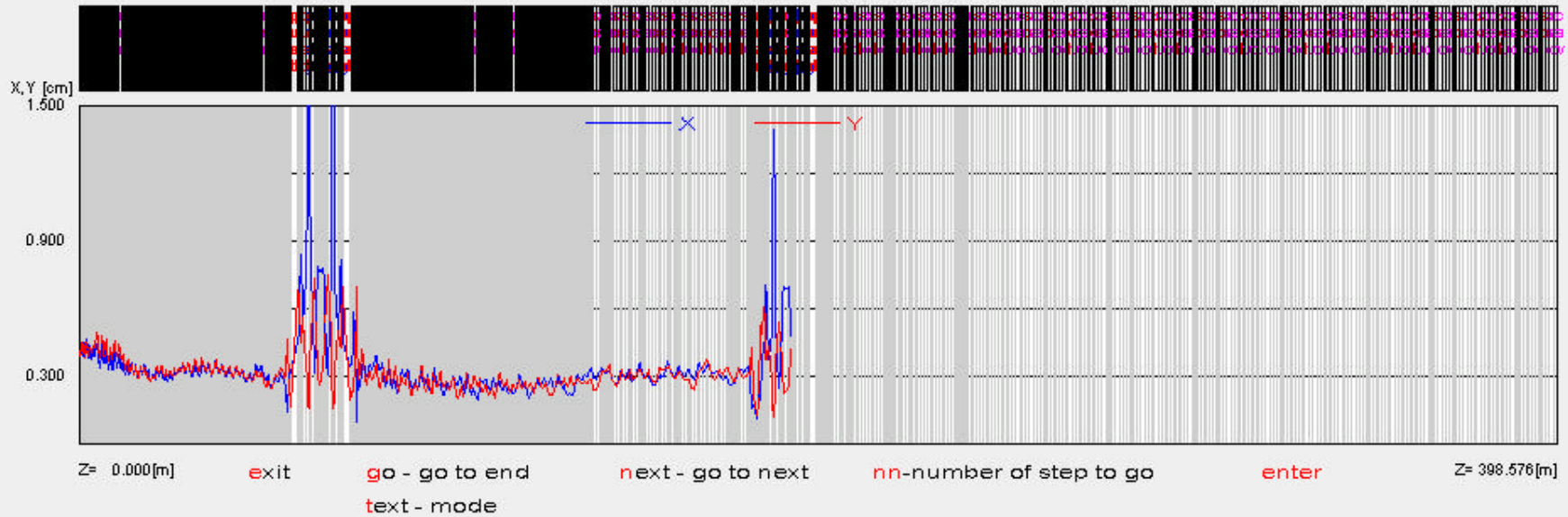
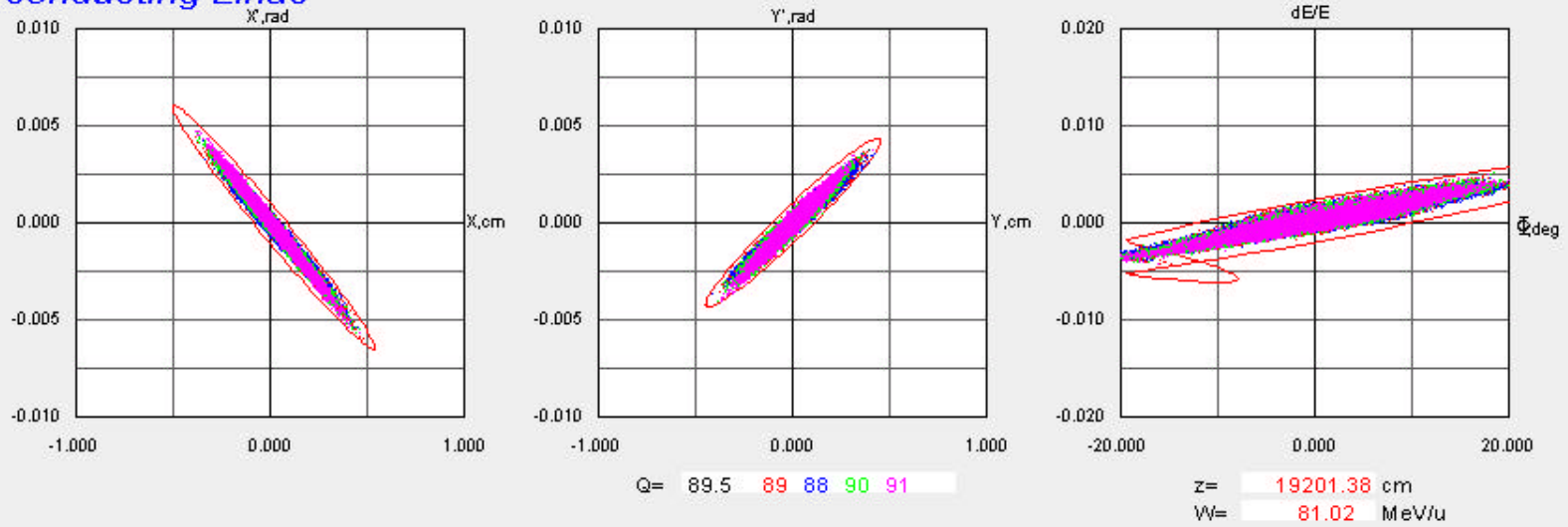
Superconducting Linac



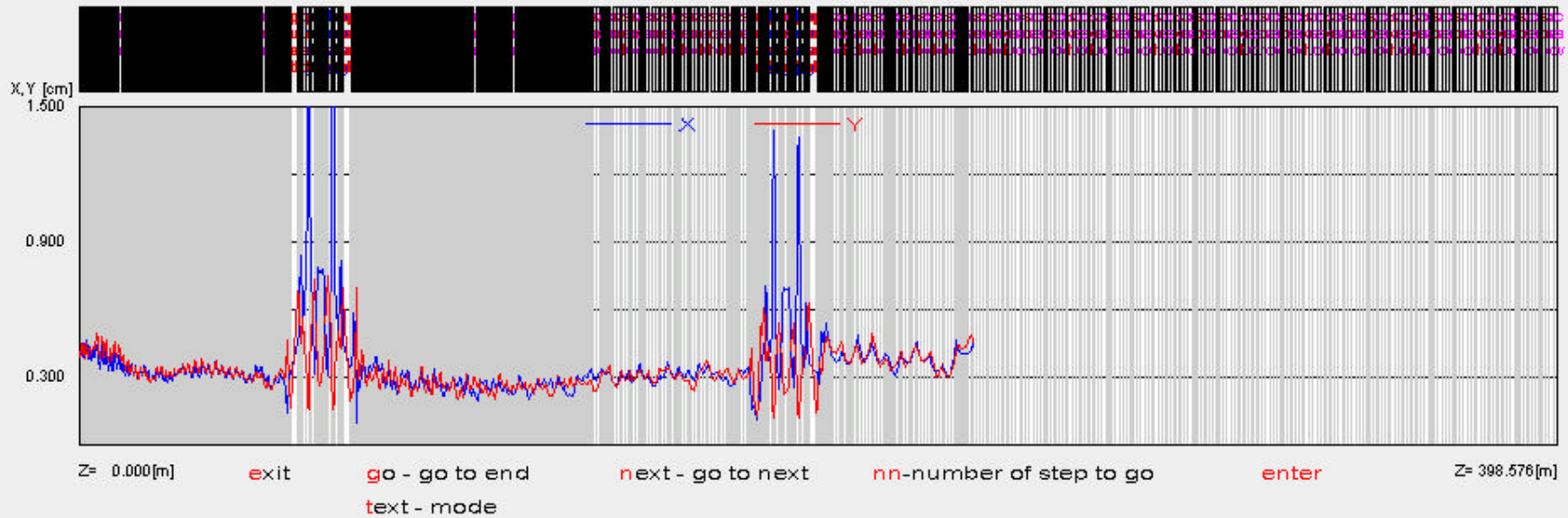
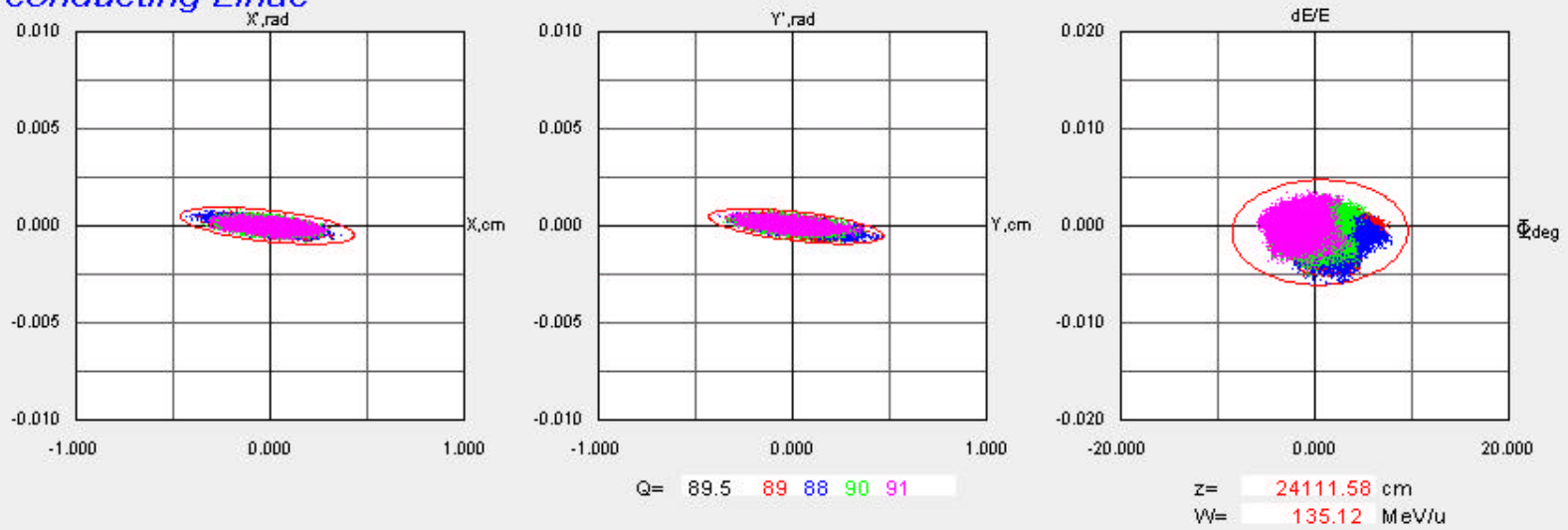
Superconducting Linac



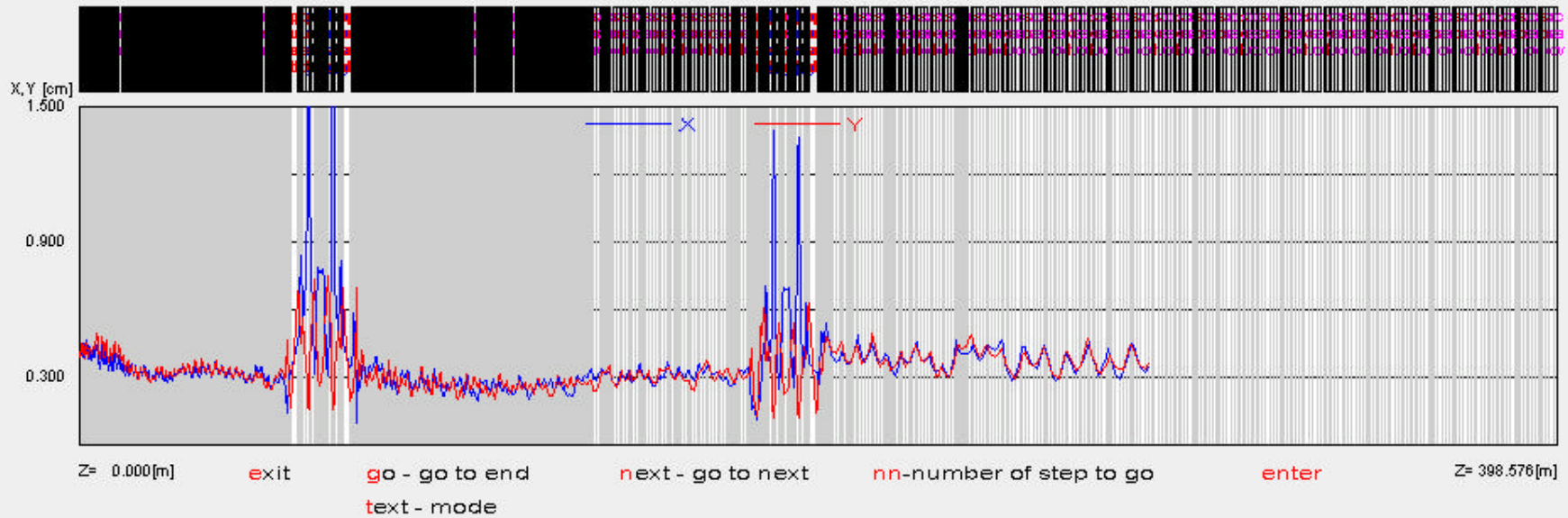
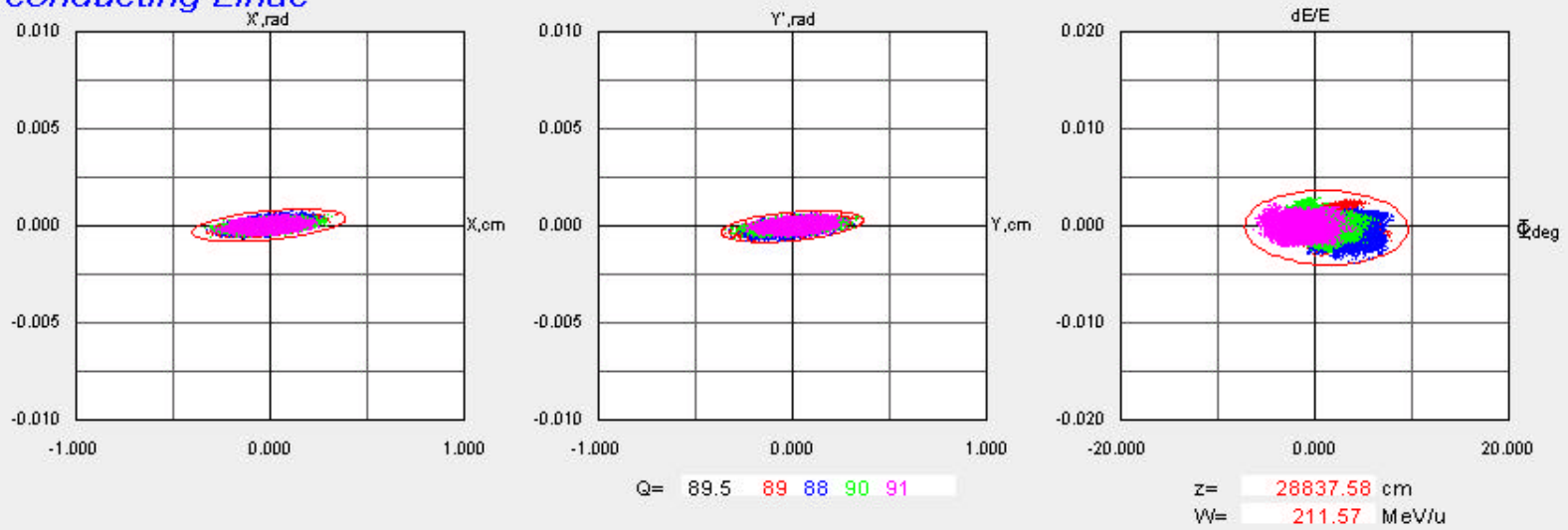
Superconducting Linac



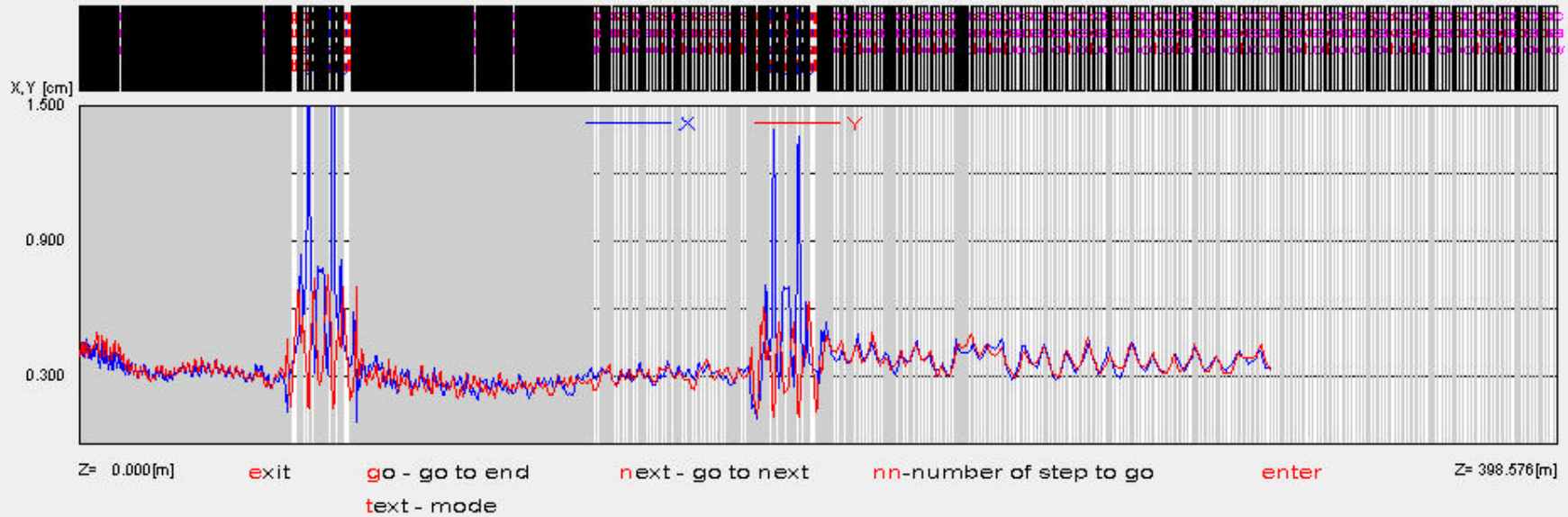
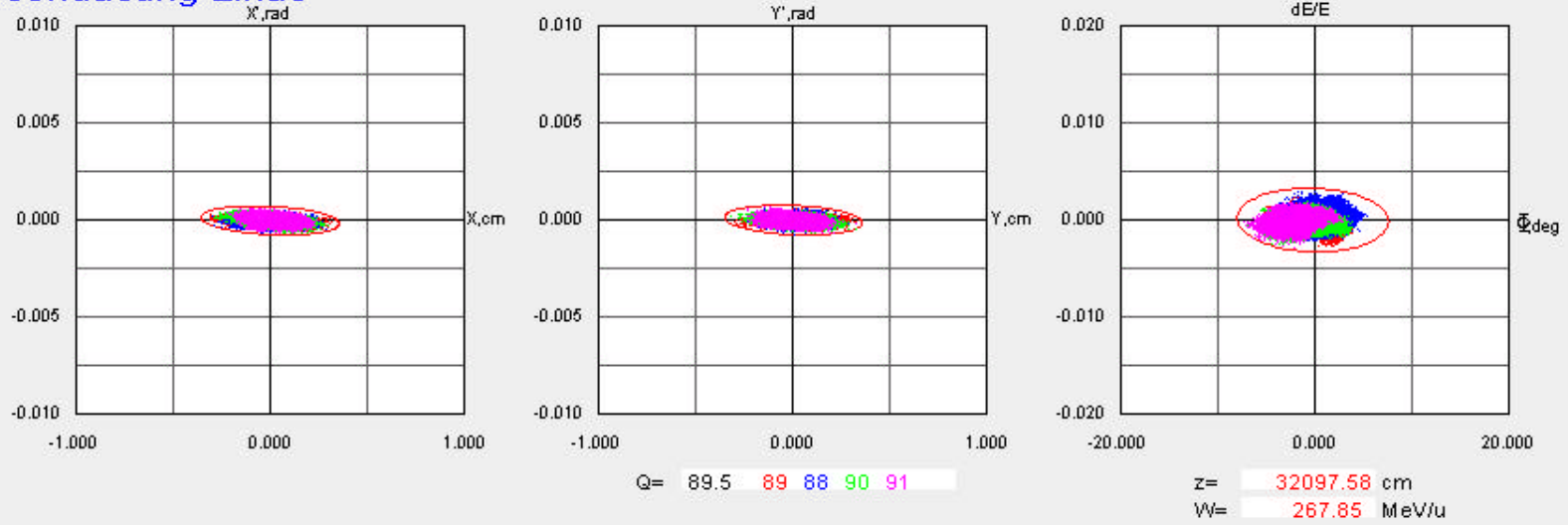
Superconducting Linac



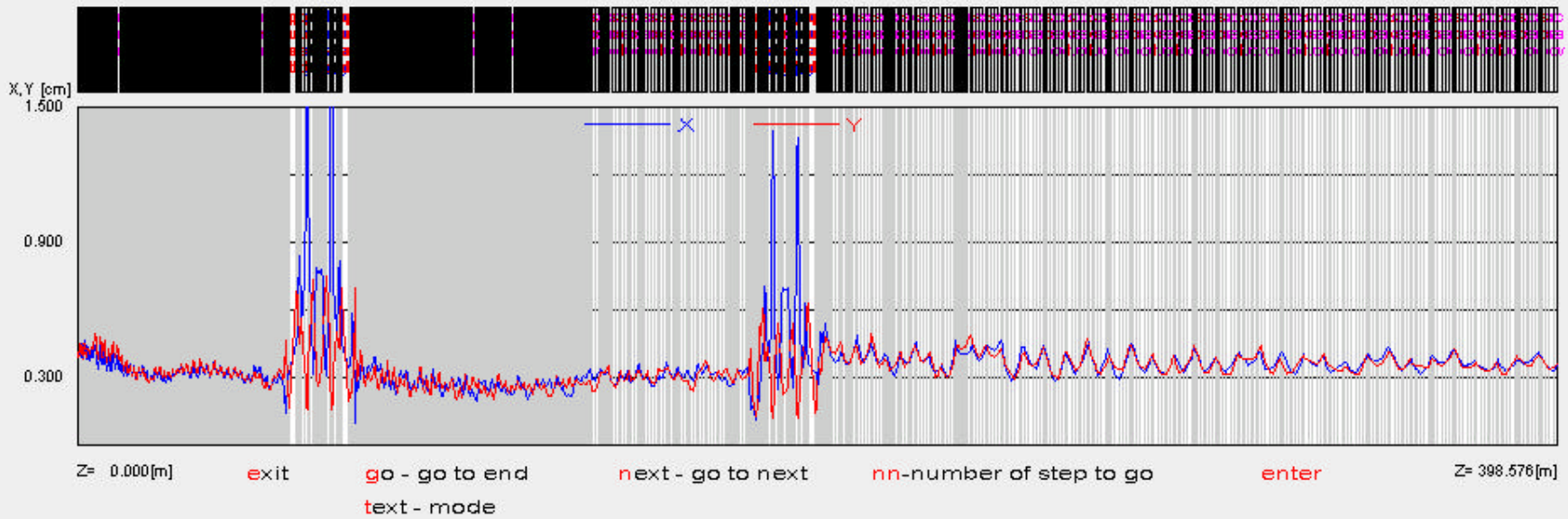
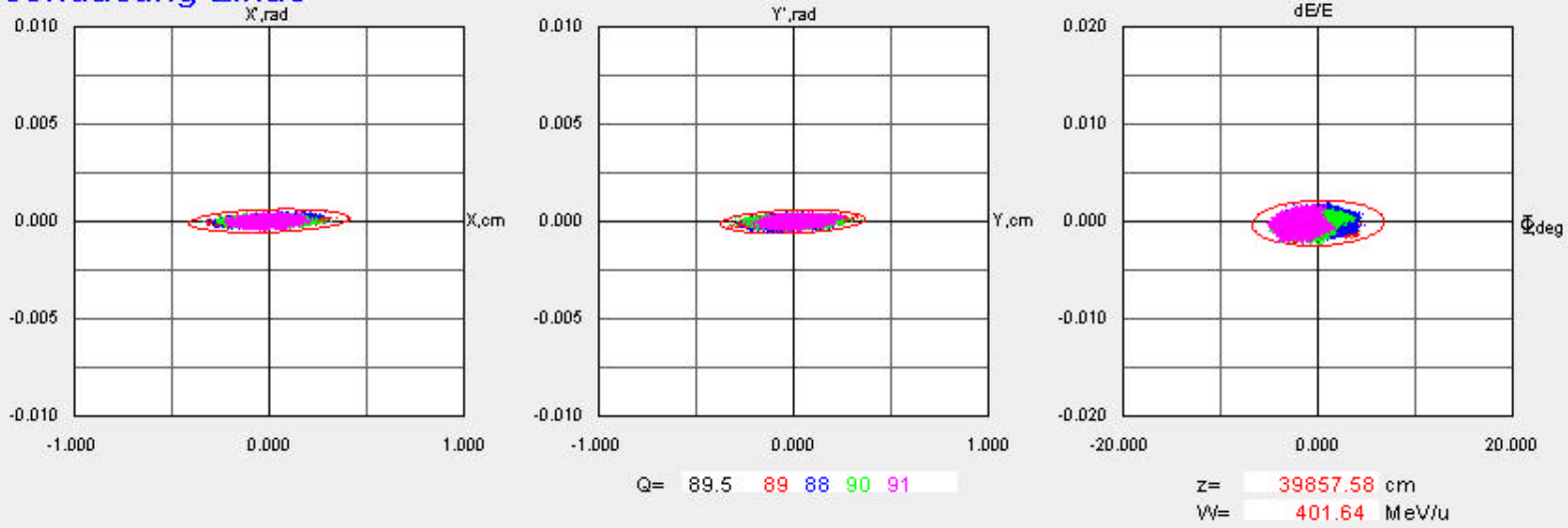
Superconducting Linac



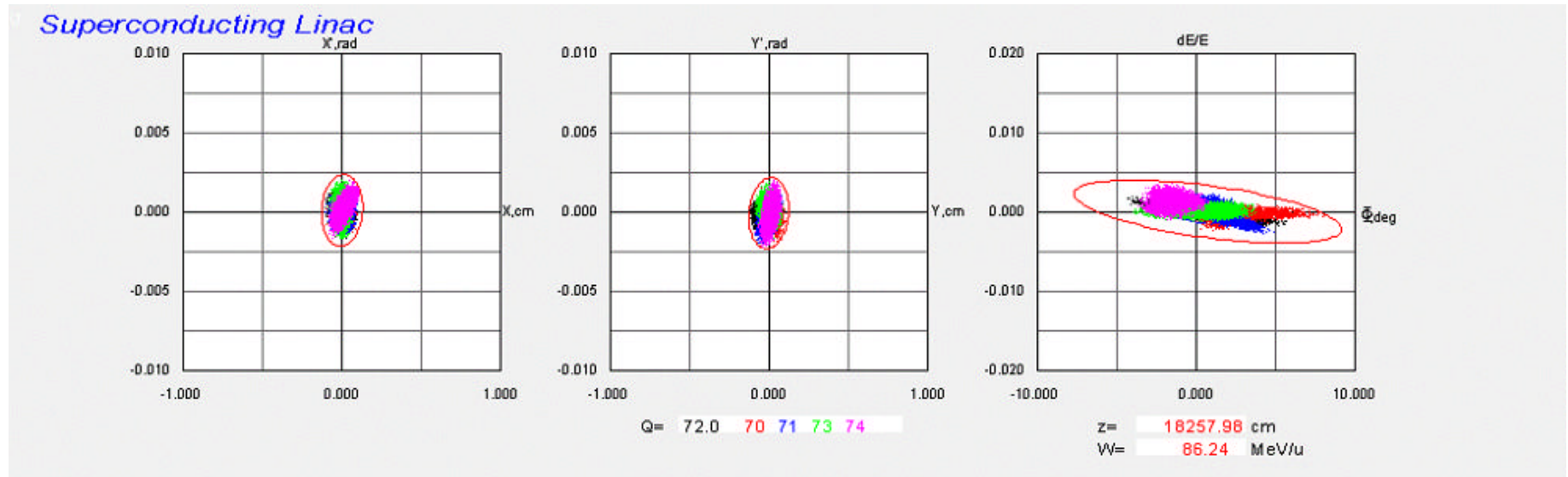
Superconducting Linac



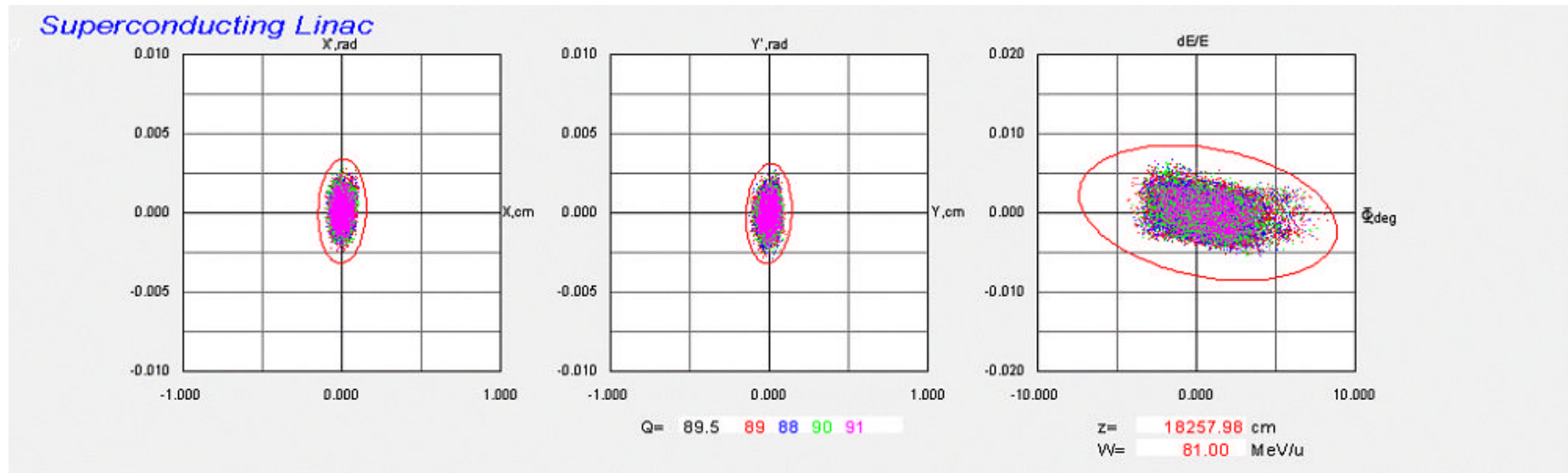
Superconducting Linac



Phase space plots before the stripper, $q=70,71,72,73,74$ ($W=85$ MeV/u)

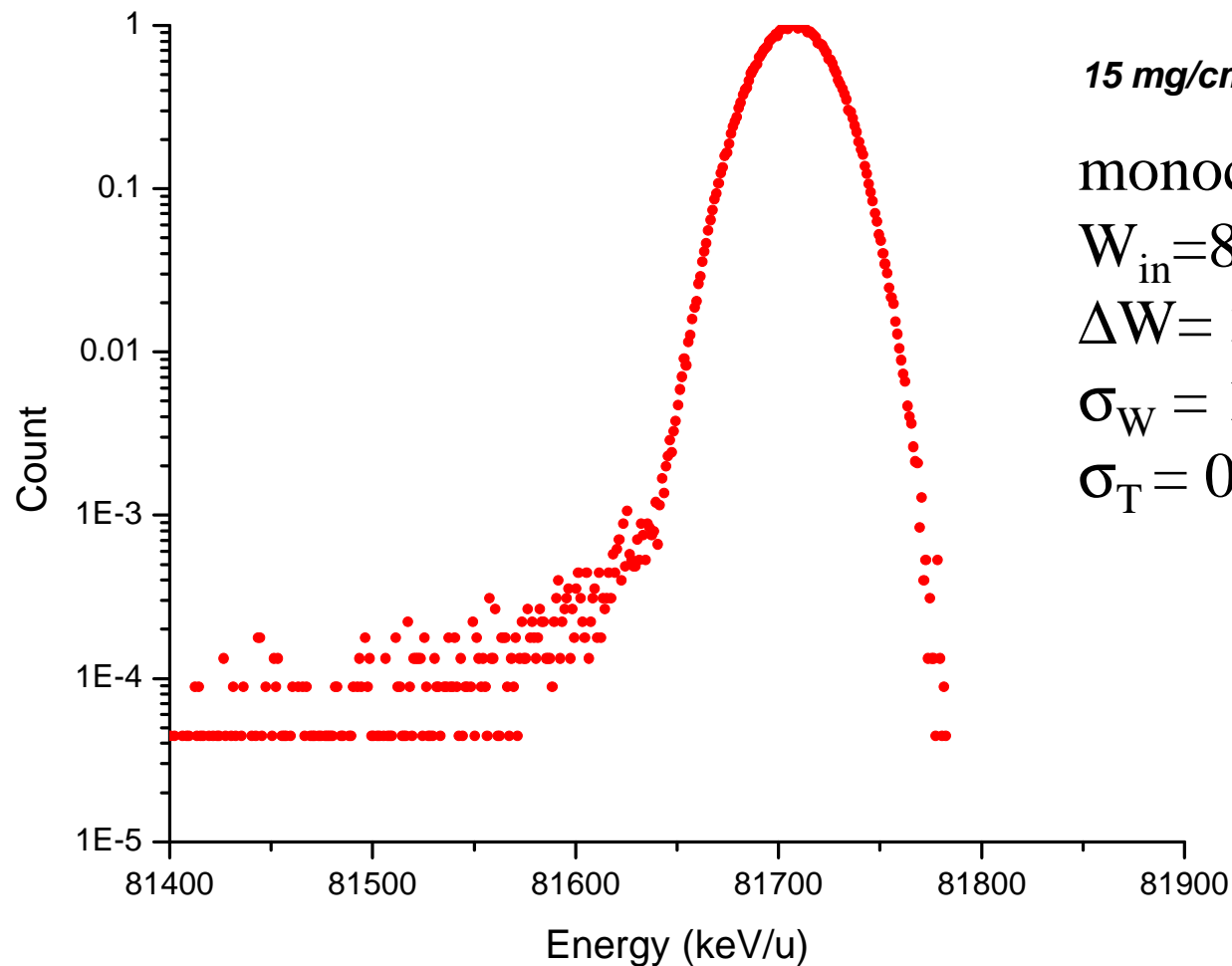


Phase space plots after the stripper, $q=88,89,90,91$ ($W=81$ MeV/u)



SRIM results, 10^6 particles

SRIM = Stopping Range of Ions in Matter
by J.F. Ziegler, J.P. Biersack and U. Littmark



15 mg/cm² Carbon foil

monochromatic input beam

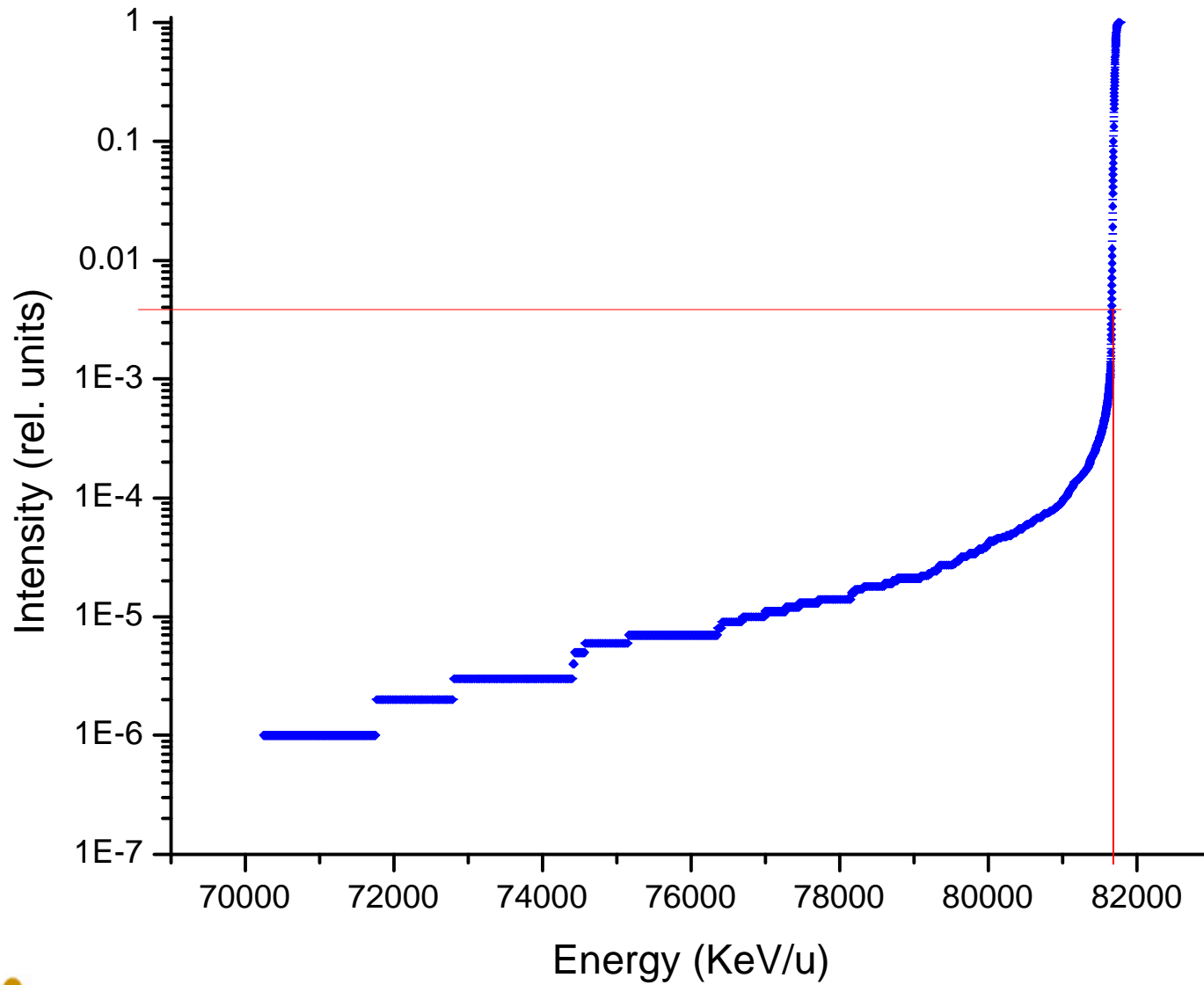
$W_{in} = 85$ MeV/u

$\Delta W = 3.29$ MeV/u

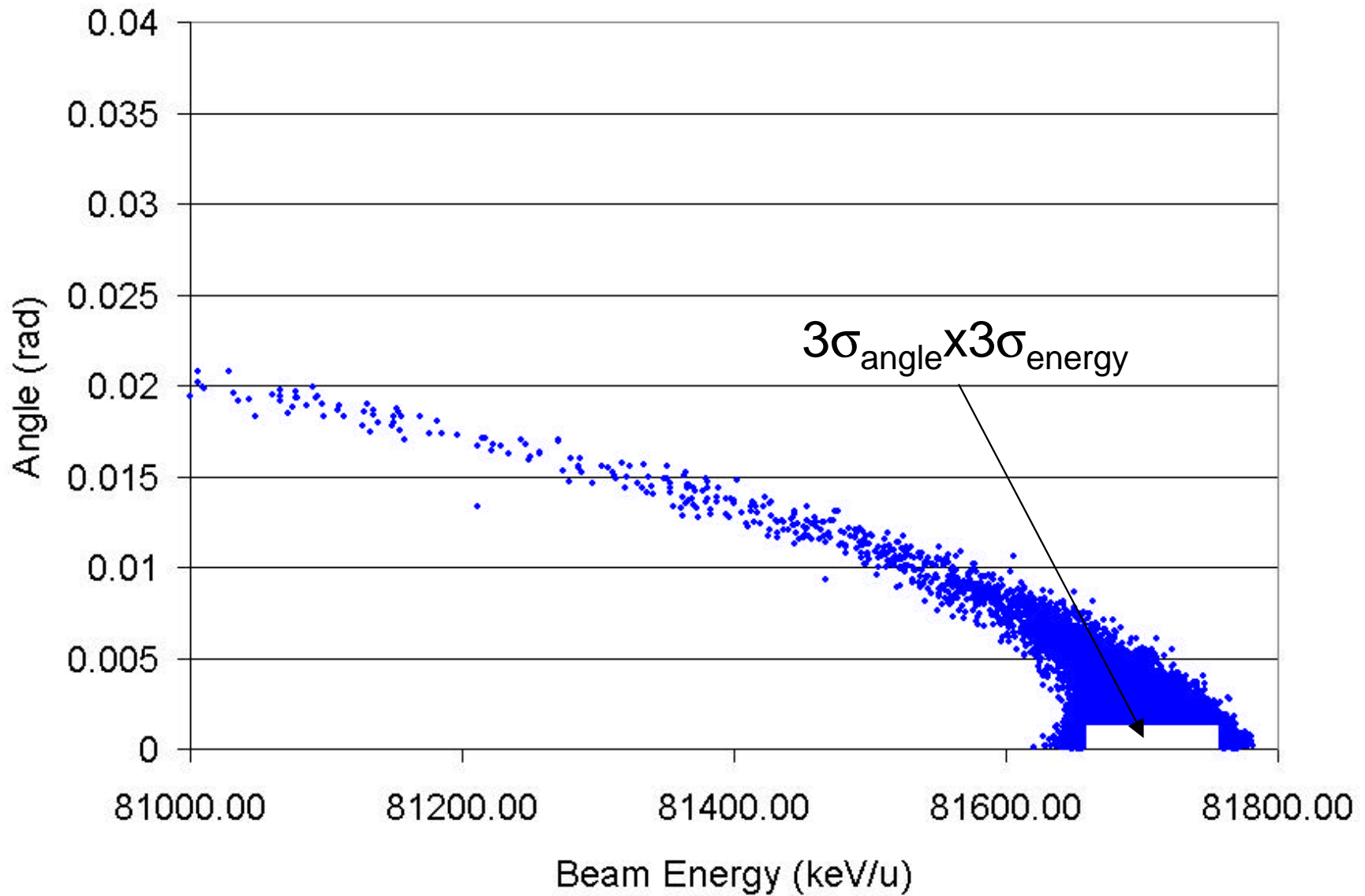
$\sigma_W = 17.5$ keV/u

$\sigma_T = 0.5$ mrad

Energy distribution function

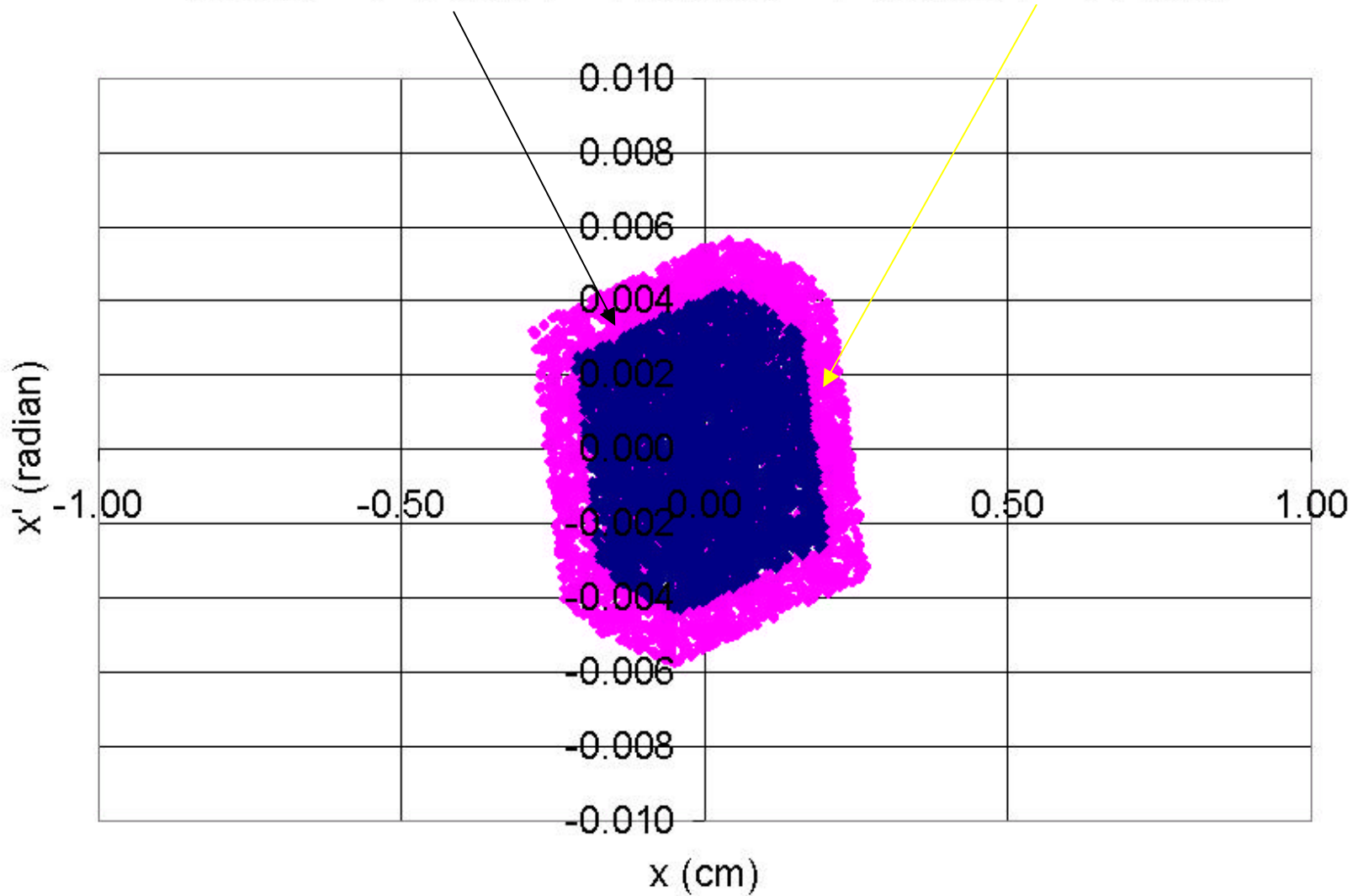


SRIM results, 10^6 particles, $\text{angle} = \sqrt{x'^2 + y'^2}$

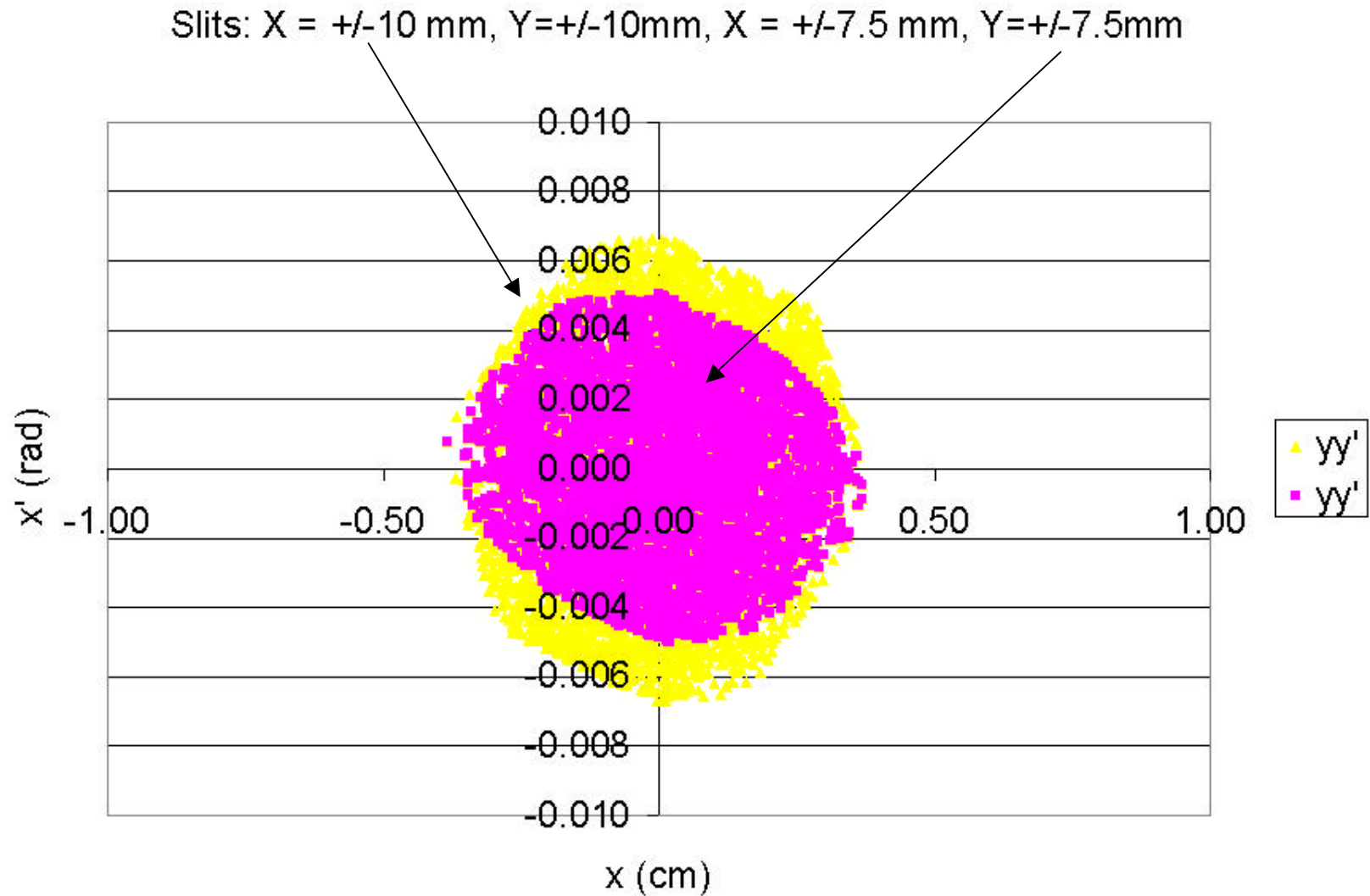


Transverse acceptance of the post-stripper MOS

Slits: X = +/- 10 mm, Y = +/- 10 mm, X = +/- 7.5 mm, Y = +/- 7.5 mm

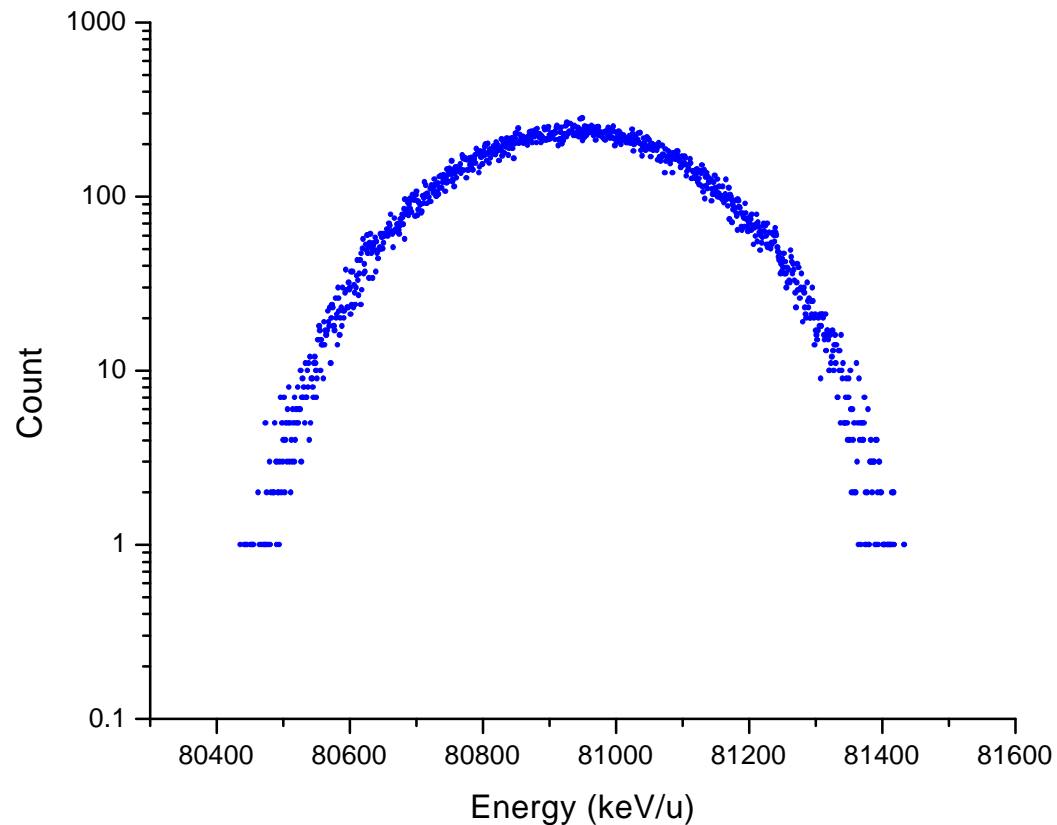


Transverse acceptance of the post-stripper MOS

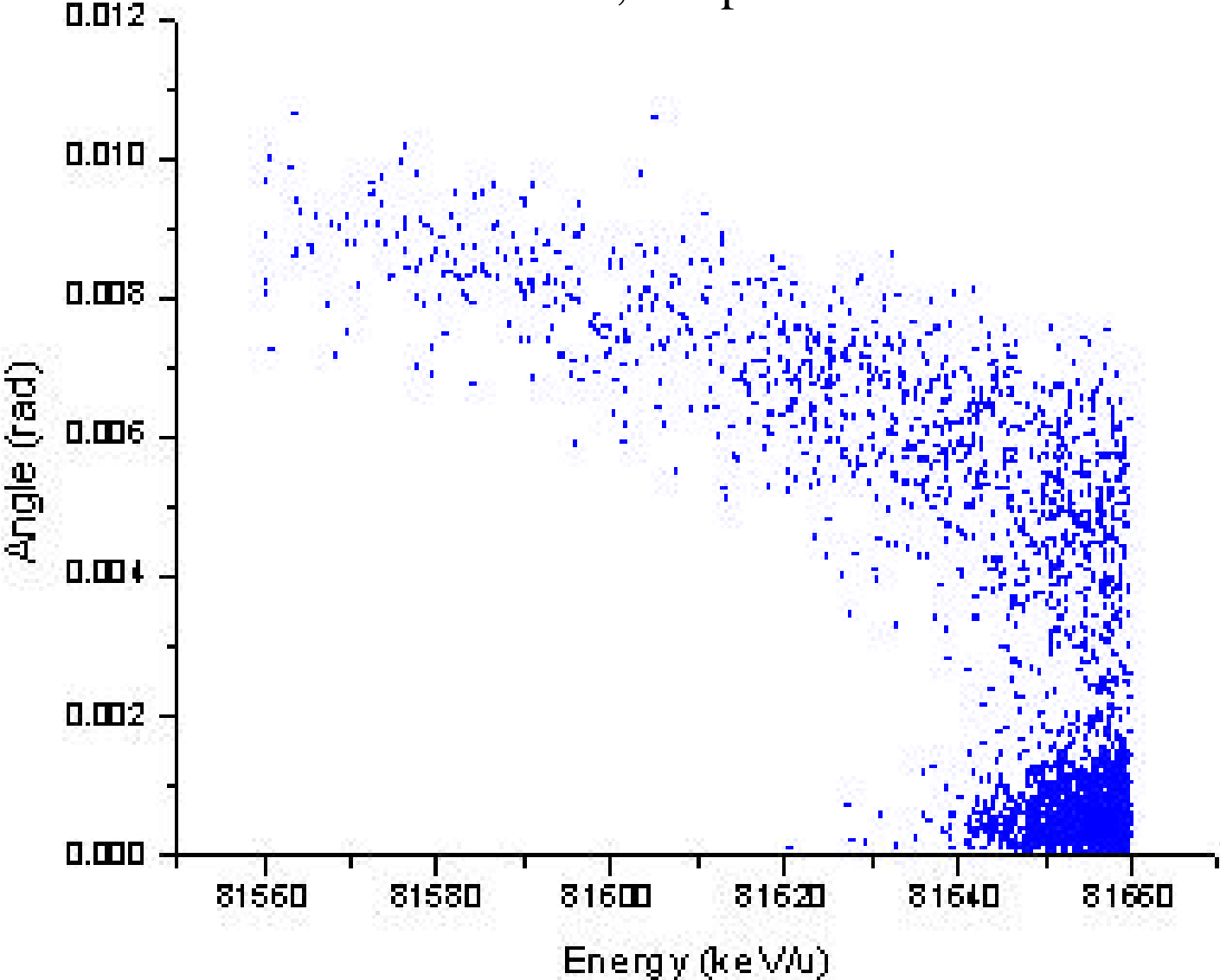


Generation of the particle distribution in TRACK, includes initial long. emittance, foil thickness fluctuation and SRIM results.

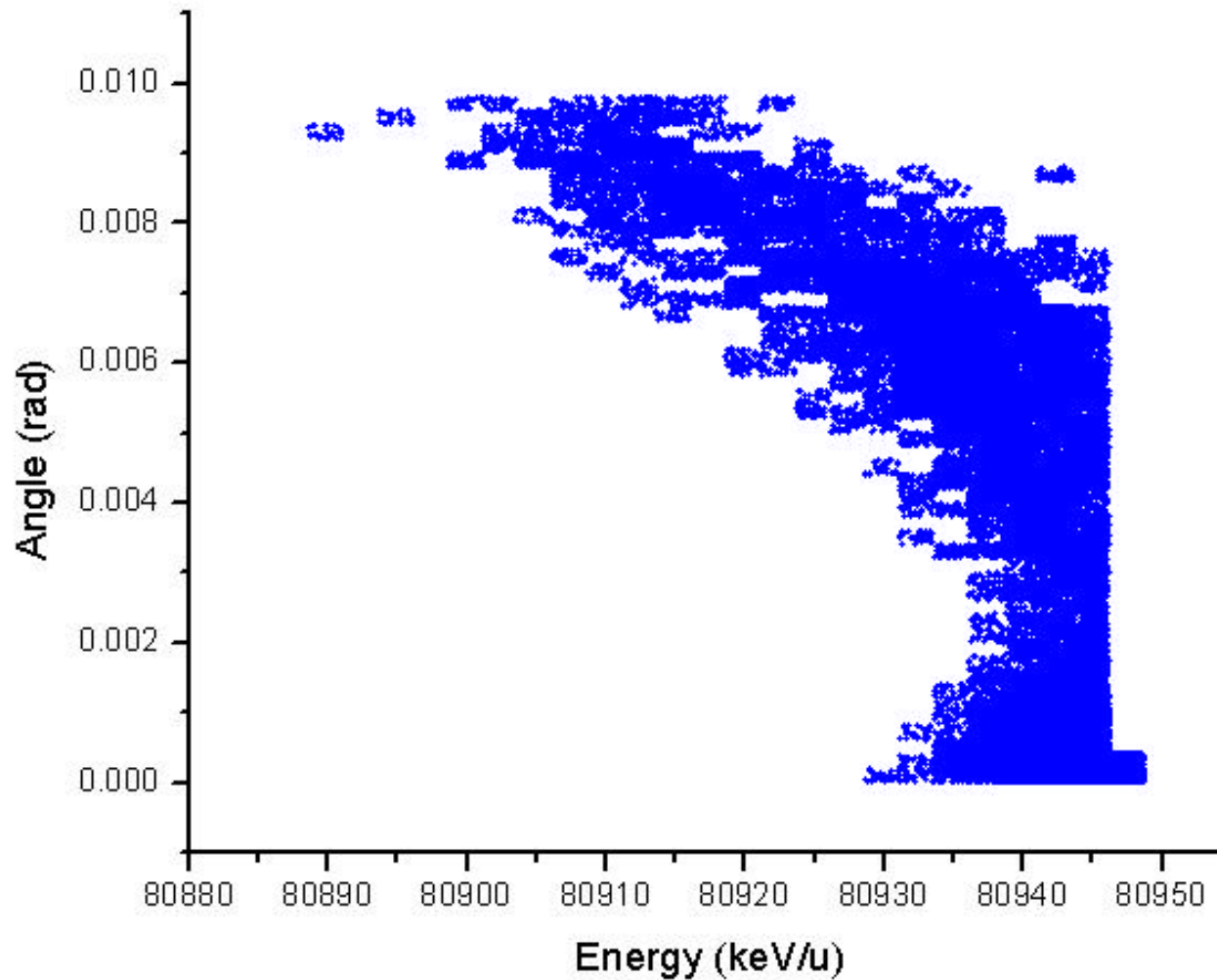
Beam core distribution in TRACK (Gaussian component)



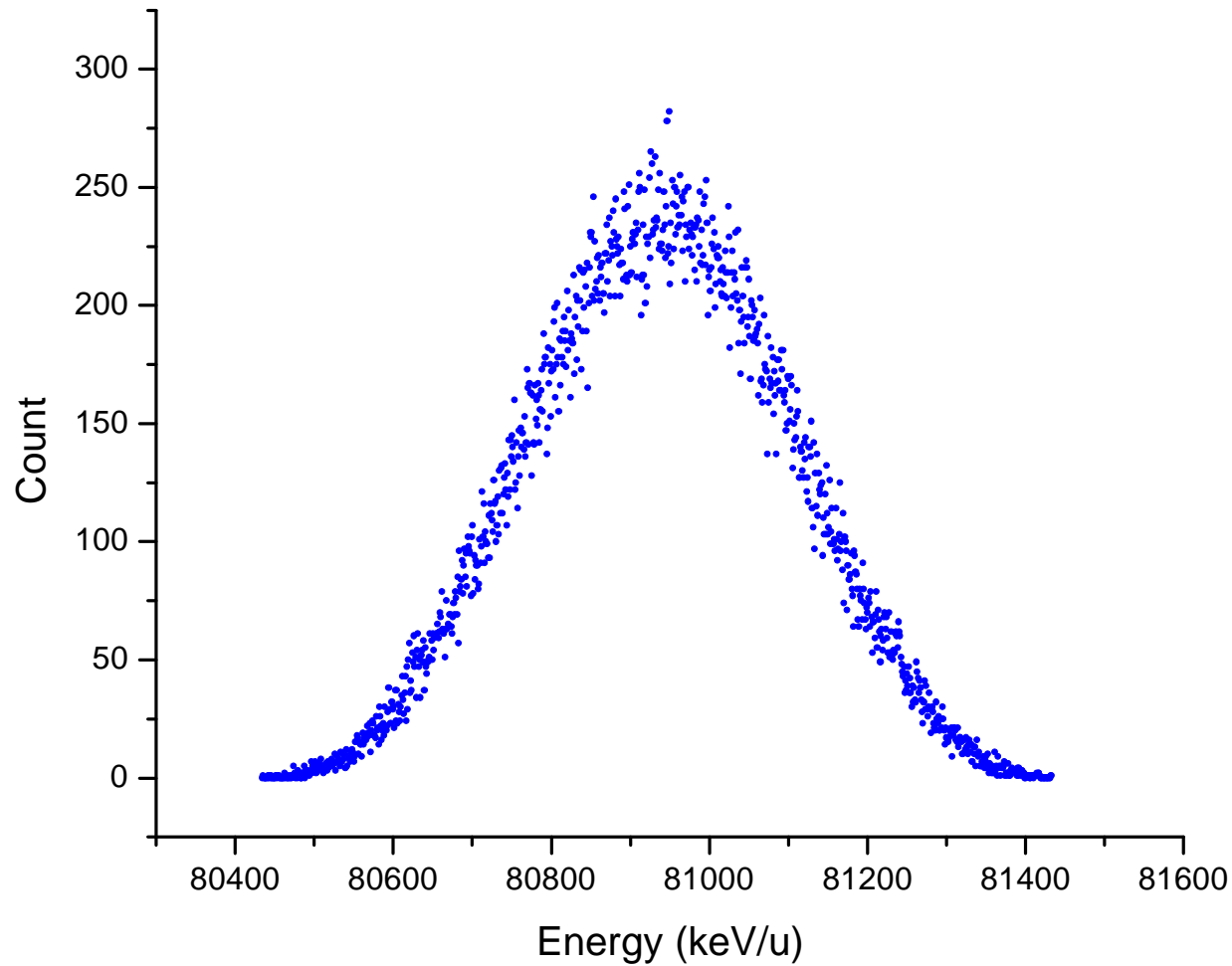
SRIM results, 10^6 particles



100,000 particles represent halo in the TRACK code:
0.3441% of total uranium beam intensity



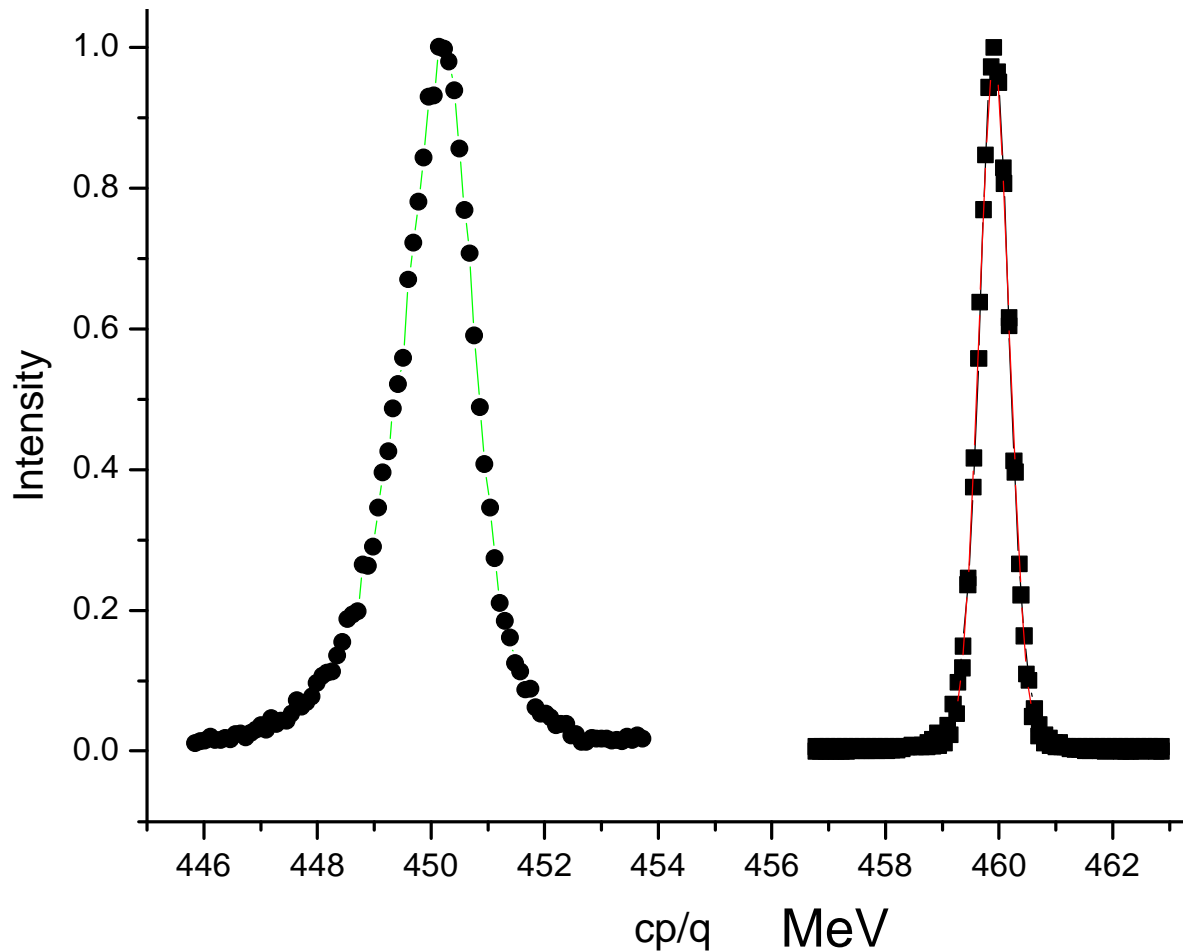
Beam energy spectrum of the halo particles (TRACK). $E_L = 29 \pi$ keV/u-nsec



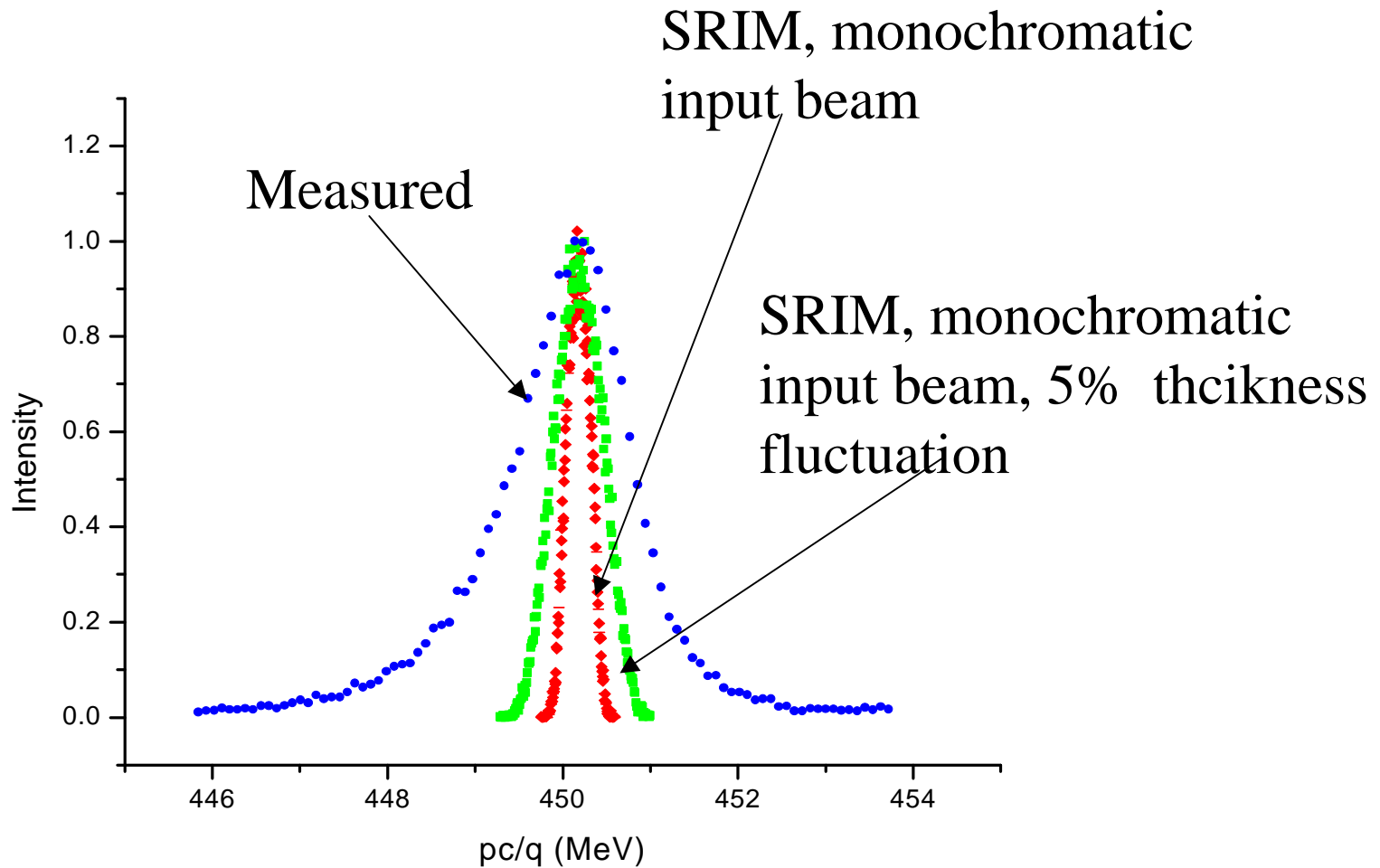
10.5 MeV/ uranium beam through C/Be foils
(measurements by J. Nolen and E. Kanter)

593 $\mu\text{g}/\text{cm}^2$ Carbon
 $\sigma=0.665$ MeV

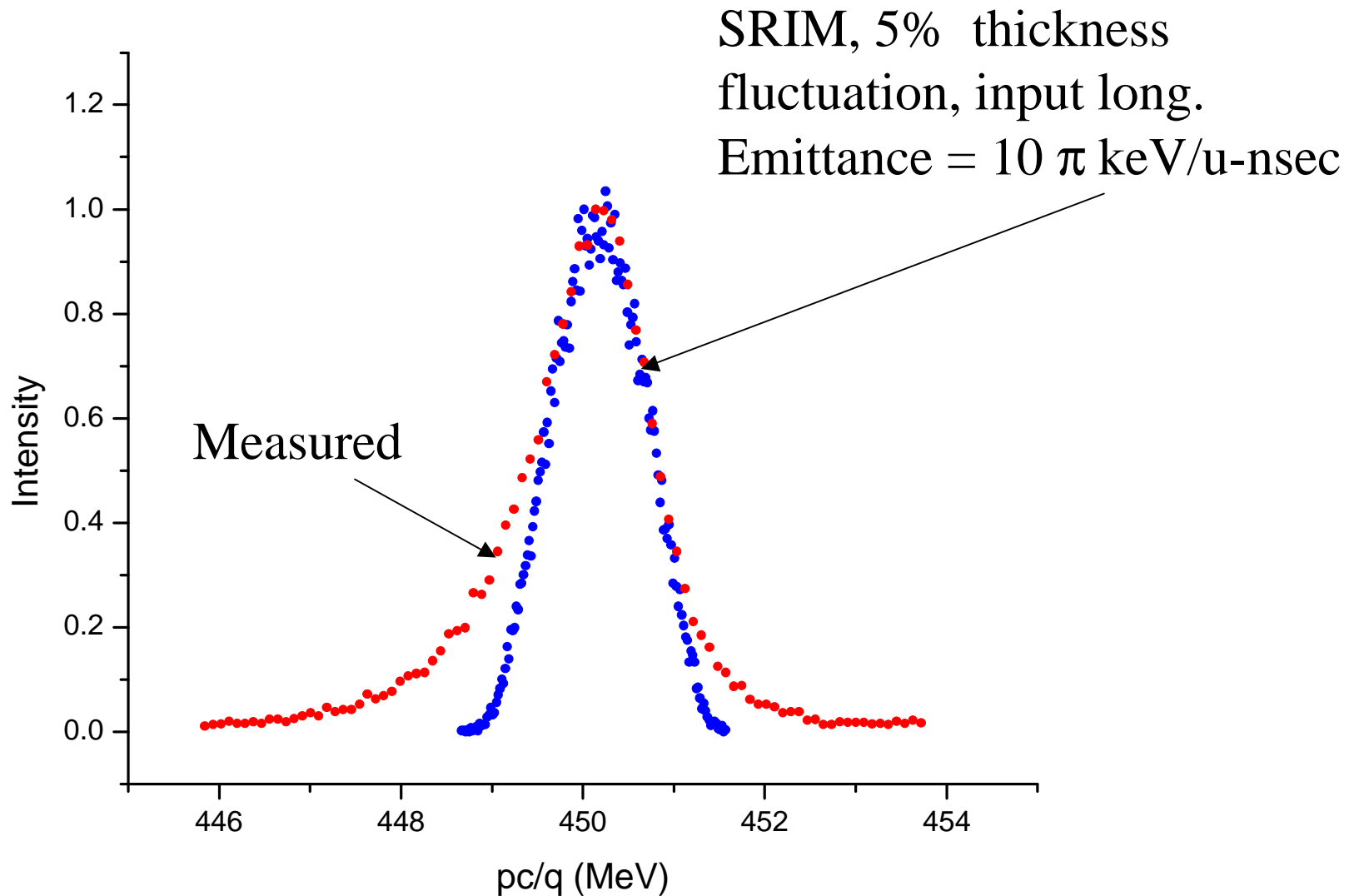
52 $\mu\text{g}/\text{cm}^2$ C and 220 $\mu\text{g}/\text{cm}^2$ Be
 $\sigma=0.27$ MeV



593 $\mu\text{g}/\text{cm}^2$ Carbon
 $s=0.665$ MeV

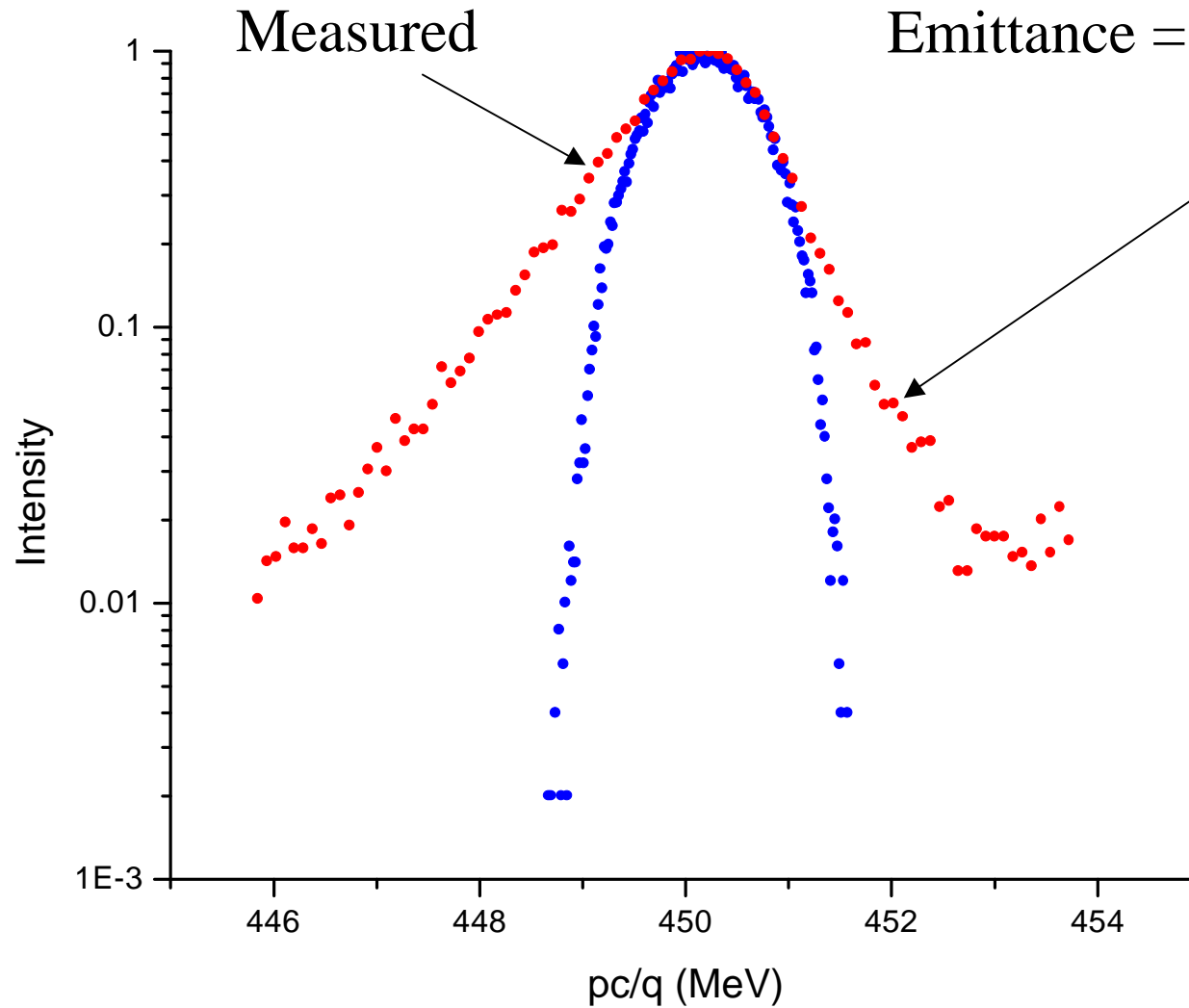


593 $\mu\text{g}/\text{cm}^2$ Carbon
 $\sigma=0.665$ MeV



593 $\mu\text{g}/\text{cm}^2$ Carbon
 $\sigma=0.665$ MeV

SRIM, 5% thickness
fluctuation, input long.
Emittance = 10π keV/u-nsec



593 $\mu\text{g}/\text{cm}^2$ Carbon

Measurement

$$\sigma_{\text{cp/q}} = 0.55 \text{ MeV}$$

SRIM Simulation

$$\sigma_{\text{cp/q}} = 0.064 \text{ MeV}$$

$$\sigma_{\text{W}} = 2.87 \text{ keV/u}$$

52 $\mu\text{g} / \text{cm}^2$ C and 220 $\mu\text{g} / \text{cm}^2$ Be

Measurement

$$\sigma_{\text{cp/q}} = 0.27 \text{ MeV}$$

SRIM Simulation

$$\sigma_{\text{cp/q}} = 0.04 \text{ MeV}$$

$$\sigma_{\text{W}} = 1.77 \text{ keV/u}$$

Extrapolation of energy straggling from 2 set of measurements:

$$\mathbf{s}_{\text{cp/q}} = \sqrt{\mathbf{s}_{\text{C}}^2 - \mathbf{s}_{\text{Be}}^2 - \mathbf{s}_{\text{Fluc}}^2} = \sqrt{0.55^2 - 0.27^2 - 0.206^2} = 0.43 \text{ MeV}$$

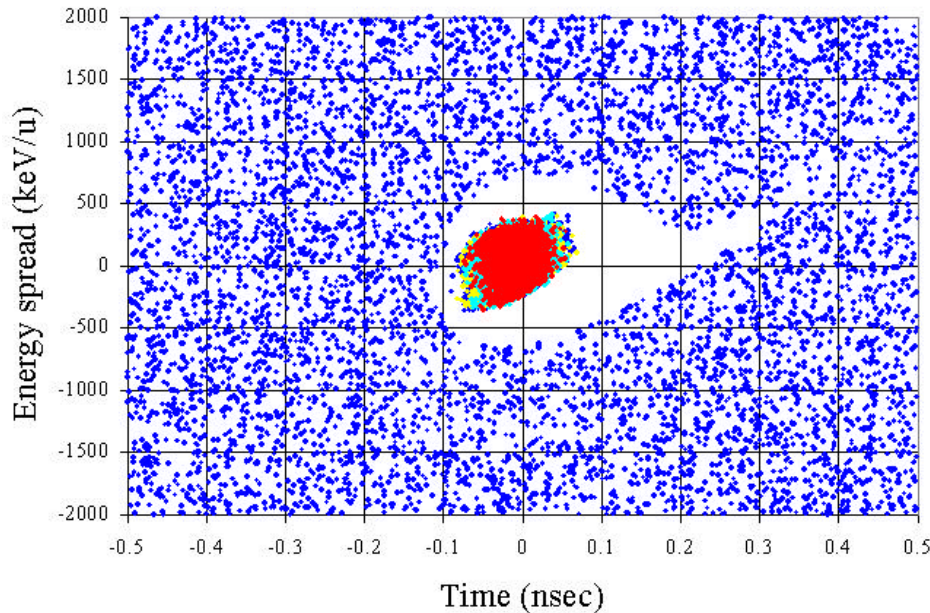
↑
±5% thickness fluc.

This is larger than SRIM data by a factor 6.7 !

Four charge state beam emittance $q=88,89,90,91$
Beam simulation to the entrance of the high- β section (no errors)

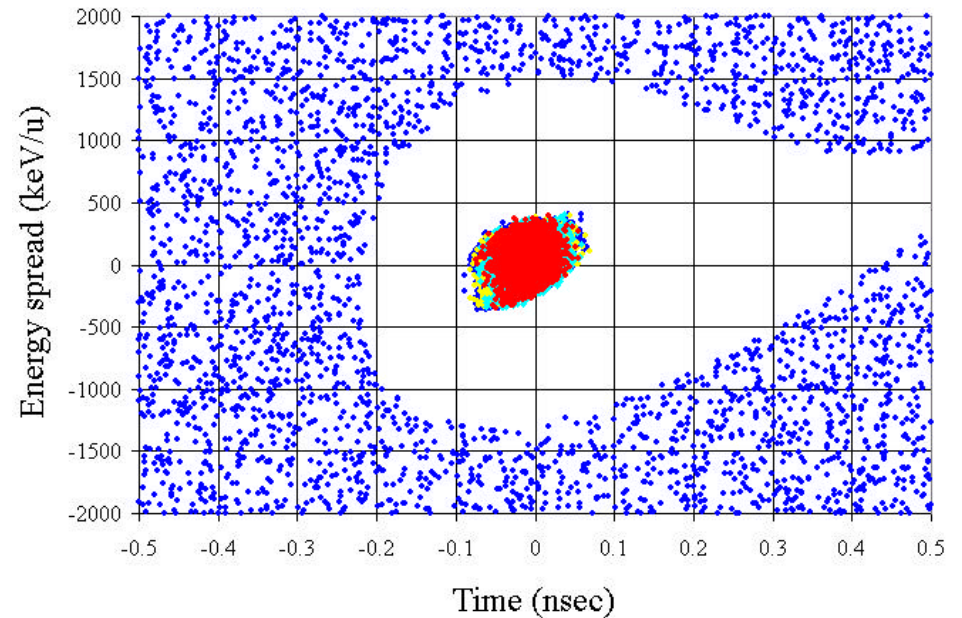
Elliptical Cavity Linac, $\varphi_S=-30^\circ$

$f=805$ MHz



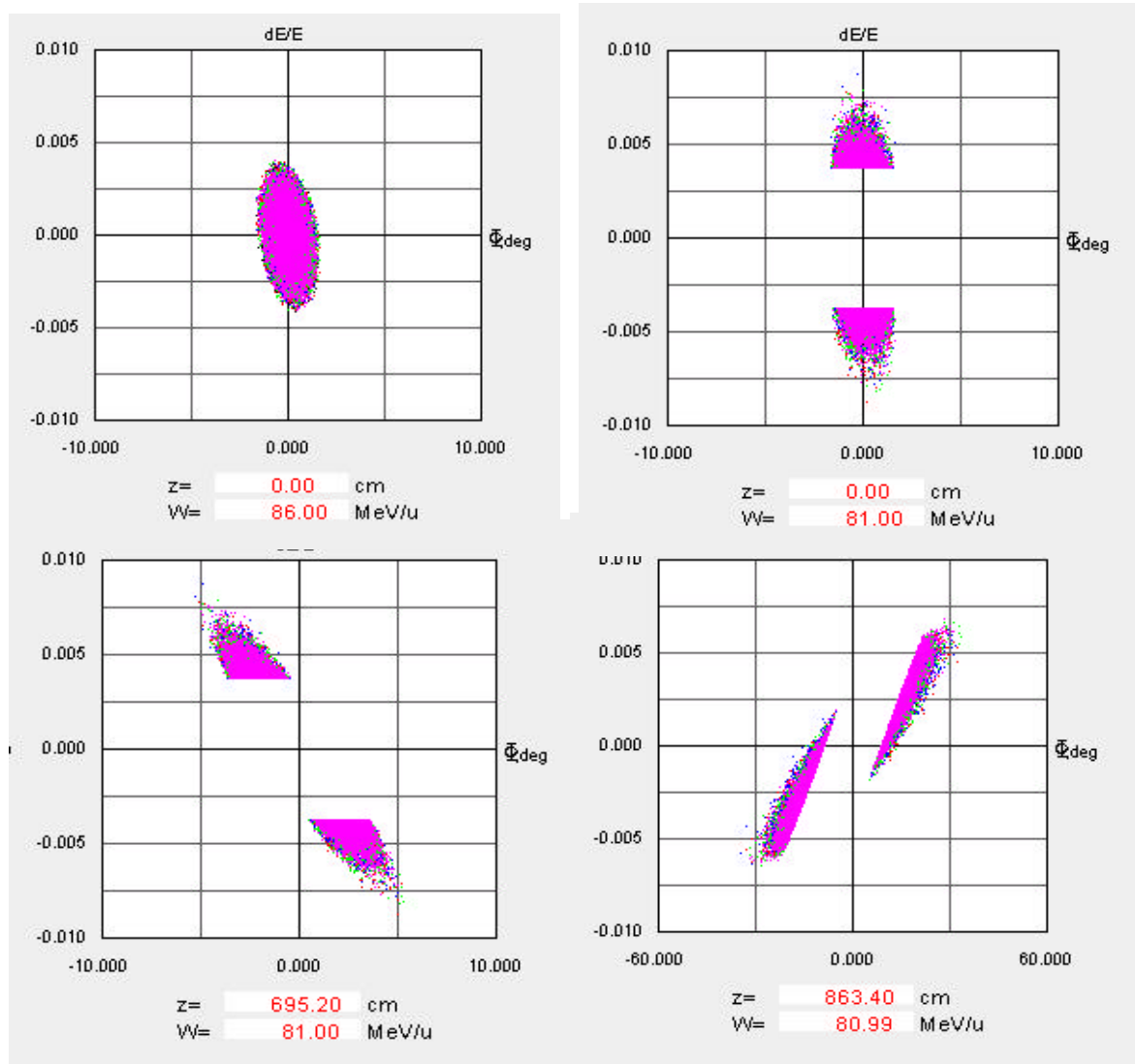
Triple Spoke Linac, $\varphi_S=-25^\circ$

$f=345$ MHz

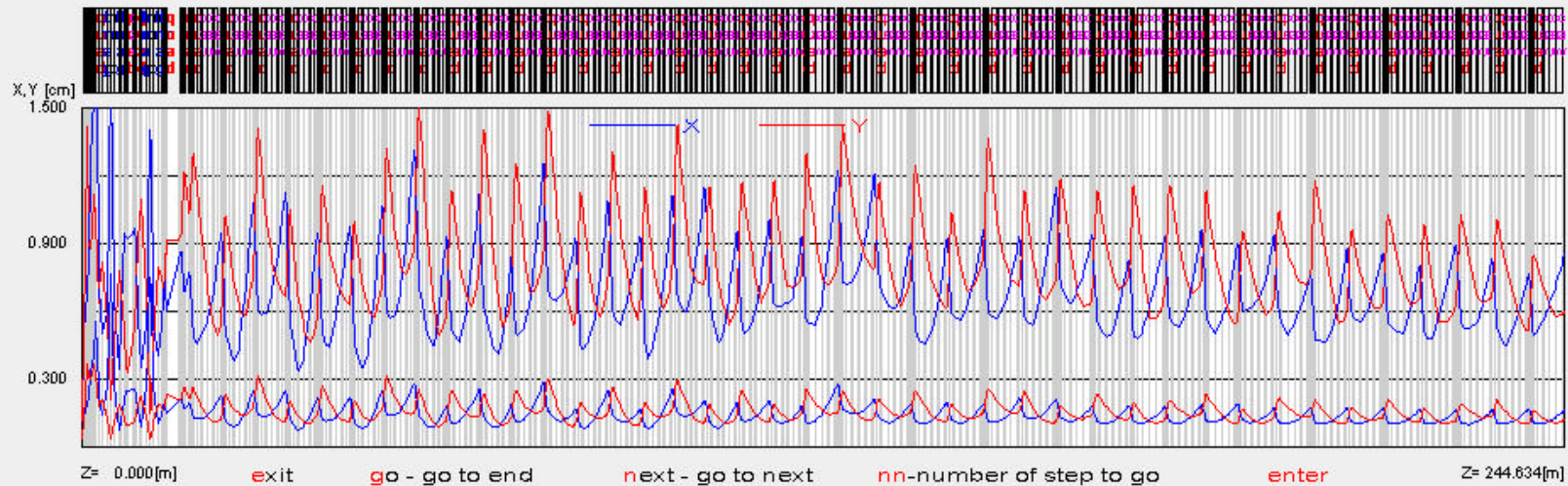
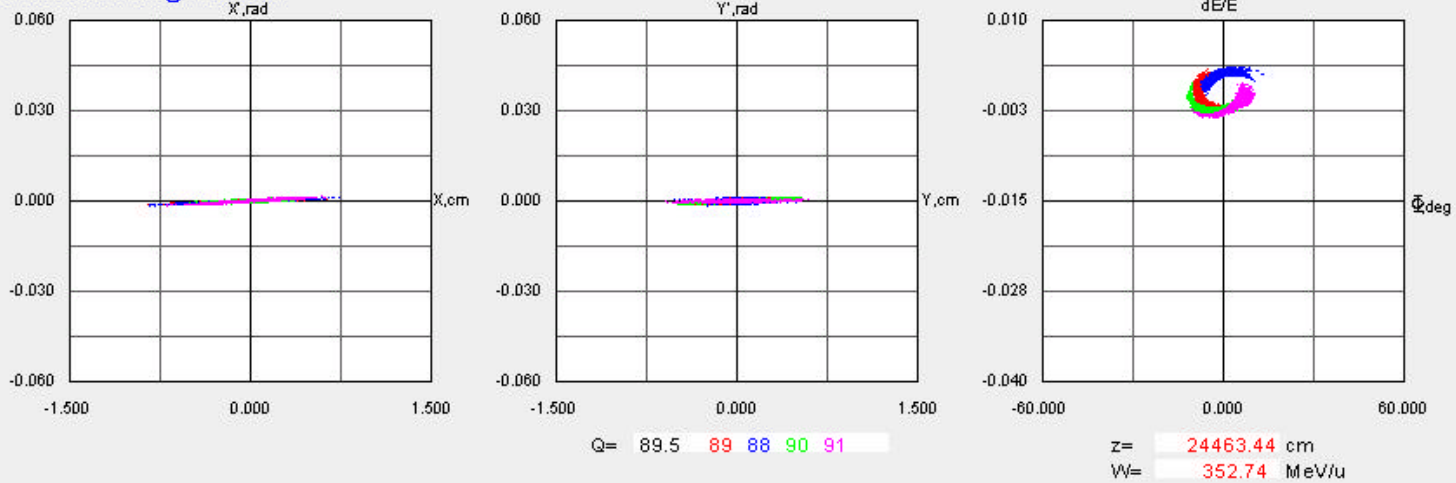


Longitudinal acceptance

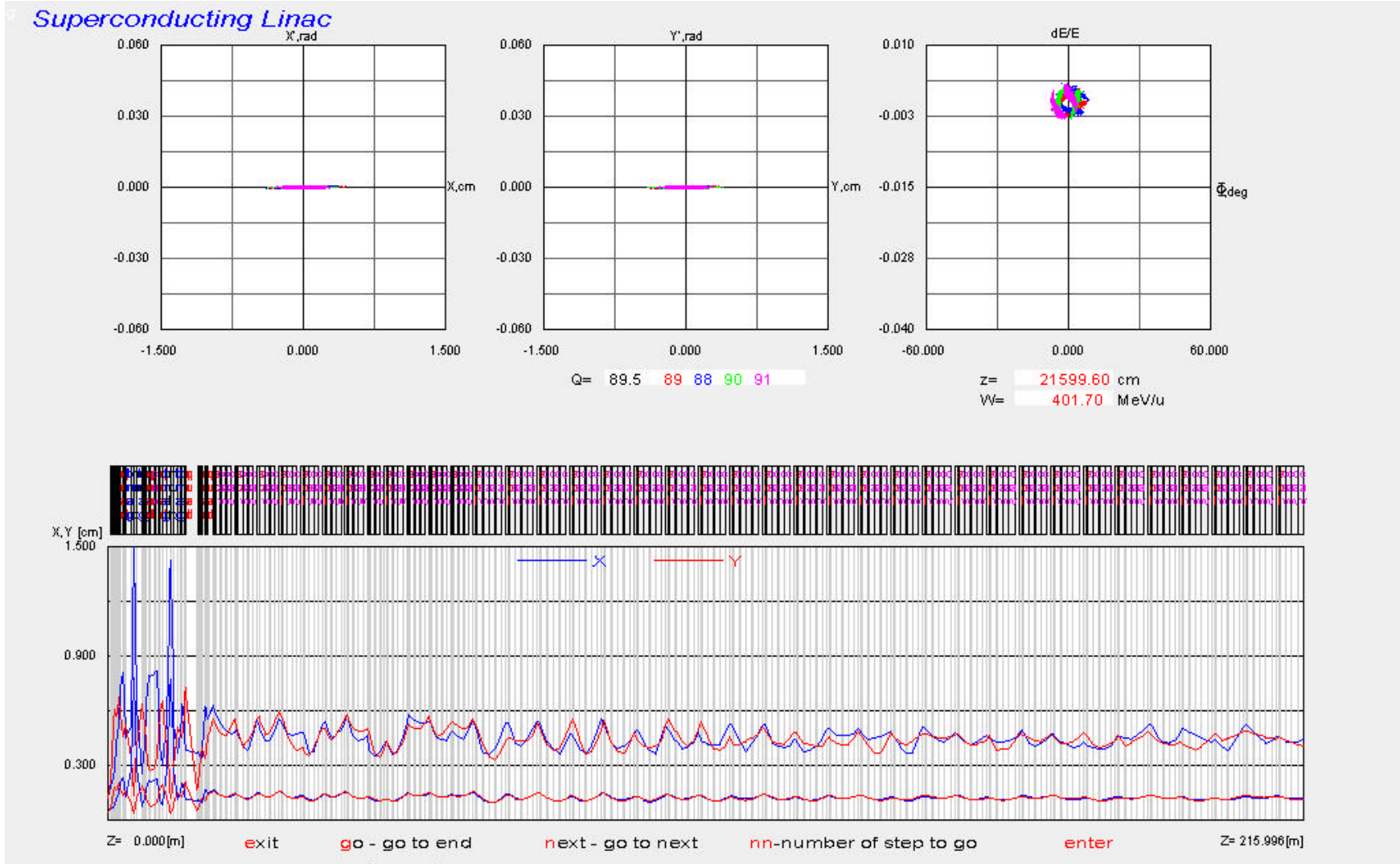
Longitudinal phase space of halo particles before the stripper and along the MOS



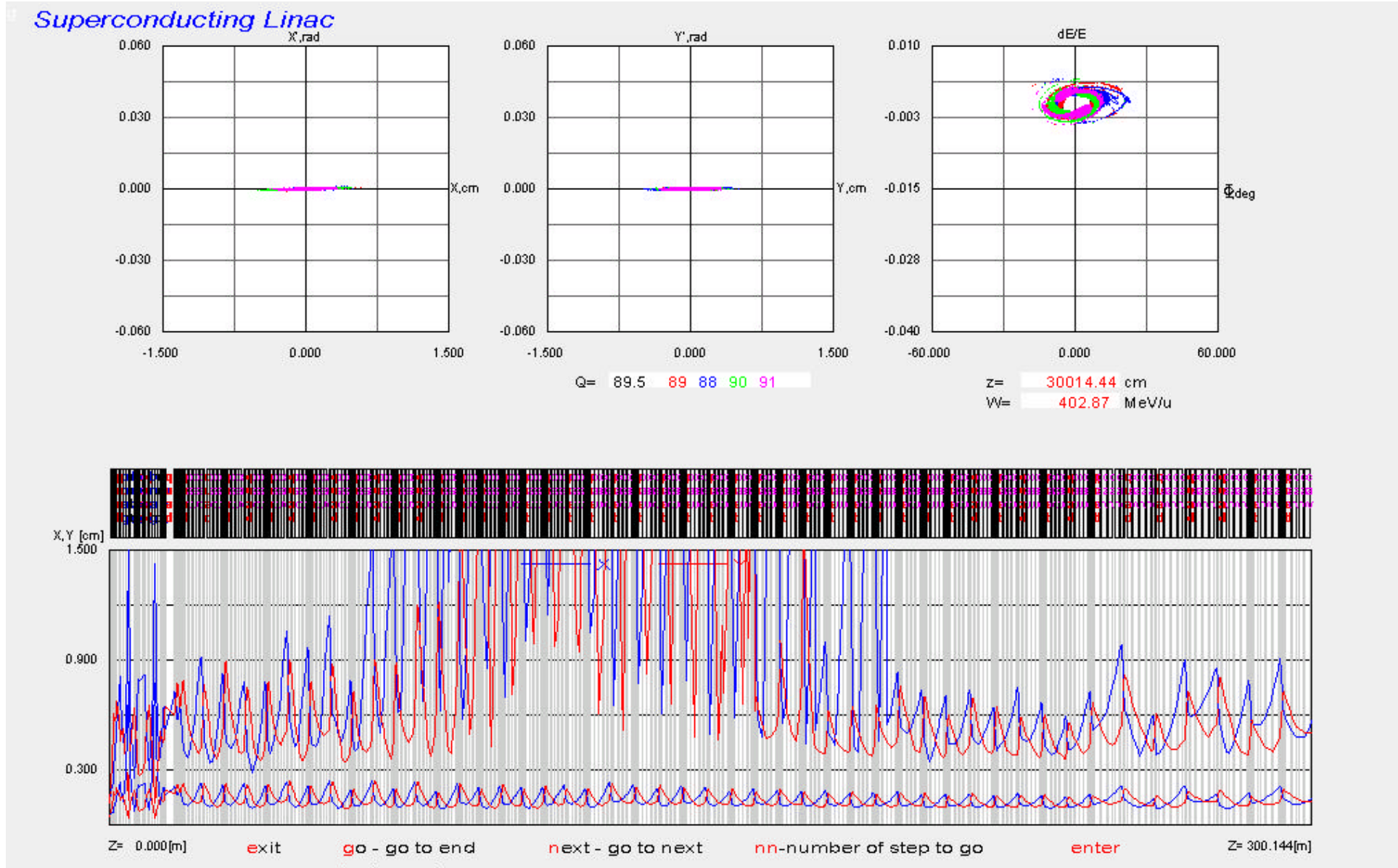
Superconducting Linac



ECL, input beam is Gaussian with $3\sigma_{\text{SRIM}}$

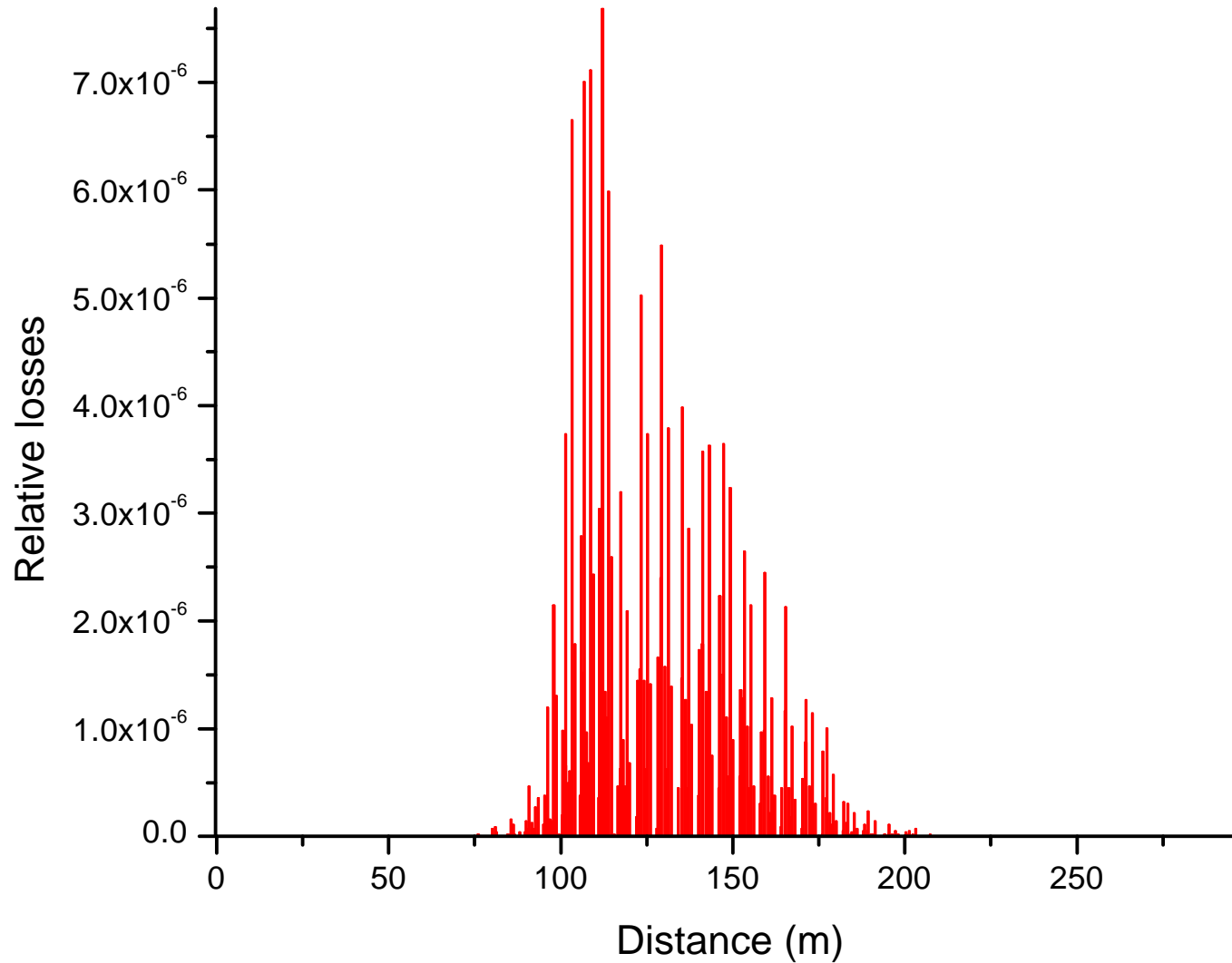


TSL, input beam is Gaussian with $5\sigma_{\text{SRIM}}$



ECL, input beam is Gaussian with $5\sigma_{\text{SRIM}}$

Distribution of particle losses along the high- β section of the ECL



Beam losses in the high energy section of the driver linac

	RF errors	ECL	TSL
σ_{SRIM} +low energy halo		no	no
$3\sigma_{\text{SRIM}}$	$\pm 0.5^\circ$ $\pm 0.5\%$	$6 \cdot 10^{-5}$	no
$5\sigma_{\text{SRIM}}$		$1.9 \cdot 10^{-4}$	no

Emittance growth factor in the RIA driver linac based on the Triple Spoke Cavities

Charge states simulated

low- β

medium- β

high- β

28-29

70-74

88-91

No errors, end-to-end simulation of 10^6 multi-particles

	Horizontal	Vertical	Longitudinal
Rms	1.5	1.5	4.9
Total (100%)	4.8	4.9	35

With errors, simulation of 10^4 multi-particles in
200 linacs with random errors and misalignments, transverse
corrective steering is applied

Rms	1.8	1.9	9.5
Total (100%)	5.8	6.8	35



Summary

SRIM data: strong correlation between the low energy particles and scattering for large angles after the passage of the stripper. Effective beam collimation can be applied along the post-stripper MOS.

Both designs of the driver linac, the ECL and TSL does not have any losses in the high energy section if SRIM results are correct. There are no losses in the TSL even for $5 \cdot \sigma_{\text{SRIM}}$. This linac is beam-loss-free .

More careful measurements of the beam energy spread and transverse emittance (or scattering angles) are required for uranium beam at 85 MeV/u.